

**Synthesis of elements 115 and 113 in the reaction  $^{243}\text{Am} + ^{48}\text{Ca}$** 

Yu. Ts. Oganessian, V. K. Utyonkov, S. N. Dmitriev, Yu. V. Lobanov, M. G. Itkis, A. N. Polyakov, Yu. S. Tsyganov, A. N. Mezentsev, A. V. Yeremin, A. A. Voinov, E. A. Sokol, G. G. Gulbekian, S. L. Bogomolov, S. Iliev, V. G. Subbotin, A. M. Sukhov, G. V. Buklanov, S. V. Shishkin, V. I. Chepygin, G. K. Vostokin, N. V. Aksenov, M. Hussonnois, K. Subotic, and V. I. Zagrebaev

*Joint Institute for Nuclear Research, RU-141980 Dubna, Russian Federation*

K. J. Moody, J. B. Patin, J. F. Wild, M. A. Stoyer, N. J. Stoyer, D. A. Shaughnessy, J. M. Kenneally, P. A. Wilk, and R. W. Lougheed

*University of California, Lawrence Livermore National Laboratory, Livermore, California 94551, USA*

H. W. Gäggeler, D. Schumann, H. Bruchertseifer, and R. Eichler

*Paul Scherrer Institute, Villigen CH-5232, Switzerland*

(Received 21 March 2005; published 29 September 2005)

The results of two experiments designed to synthesize element 115 isotopes in the  $^{243}\text{Am} + ^{48}\text{Ca}$  reaction are presented. Two new elements with atomic numbers 113 and 115 were observed for the first time. With 248-MeV  $^{48}\text{Ca}$  projectiles, we observed three similar decay chains consisting of five consecutive  $\alpha$  decays, all detected in a total time interval of 30 s. Each chain was terminated by a spontaneous fission (SF) with a high-energy release and a lifetime of about a day. With 253-MeV  $^{48}\text{Ca}$  projectiles, we registered a different decay chain of consecutive  $\alpha$  decays detected in a time interval of 0.5 s, also terminated by spontaneous fission, but after 1.8 h. The decay properties of the eleven new  $\alpha$ - and SF-decaying nuclei are consistent with expectations for consecutive  $\alpha$  decays originating from the parent isotopes  $^{288}115$  and  $^{287}115$ , produced in the  $3n$ - and  $4n$ -evaporation channels, respectively. Support for the assignment of the atomic numbers of all of the nuclei in the  $^{288}115$  decay chain was obtained in an independent experiment in which a long-lived spontaneous fission activity,  $^{268}\text{Db}$  (15 events), was found to be chemically consistent with the fifth group of the periodic table. The odd-odd isotope  $^{288}115$  was observed with largest cross section of about 4 pb. In the SF decay of  $^{268}\text{Db}$ , a total kinetic energy of 230 MeV and a neutron multiplicity per fission of 4.2 were measured. The decay properties of the 11 new isotopes with  $Z = 105$ –115 and the production cross sections are in agreement with modern concepts of the role of nuclear shells in the stability of superheavy nuclei. The experiments were carried out at the Flerov Laboratory of Nuclear Reactions, Joint Institute for Nuclear Research.

DOI: [10.1103/PhysRevC.72.034611](https://doi.org/10.1103/PhysRevC.72.034611)

PACS number(s): 25.70.Gh, 23.60.+e, 25.85.Ca, 27.90.+b

**I. INTRODUCTION**

One of the fundamental outcomes of the nuclear shell model is the prediction of the existence of the “Island of Stability” in the domain of the superheavy elements. A considerable increase in nuclear stability was expected for the heaviest neutron-rich nuclei with  $N > 170$  in the vicinity of the closed spherical shells,  $Z = 114$  (or possibly 120, 122, or 126) and  $N = 184$ , similar to the effect of the closed shells on the stability of doubly magic  $^{208}\text{Pb}$  ( $Z = 82$  and  $N = 126$ ). Therefore, our first experiments aimed at the synthesis of the heaviest nuclei involved the complete fusion reactions of long-lived even- $Z$  target nuclei  $^{242,244}\text{Pu}$  and  $^{248}\text{Cm}$  with  $^{48}\text{Ca}$  projectiles leading to the compound nuclei  $^{290}114$  ( $N = 176$ ),  $^{292}114$  ( $N = 178$ ), and  $^{296}116$  ( $N = 180$ ) with the maximum accessible neutron-richness [1,2]. The isotopes of elements 114 and 116 with  $N = 172$ –177 produced in these reactions decay primarily through  $\alpha$  emission ( $T_\alpha < T_{\text{SF}}$ ). The decay chains of consecutive  $\alpha$  emissions are terminated by the spontaneous fission (SF) of descendant even-even or even-odd nuclei with  $Z = 112$  or 110 ( $T_\alpha > T_{\text{SF}}$ ).

For the neighboring odd- $Z$  elements, especially their odd-odd isotopes, the probability of  $\alpha$  decay with respect to

spontaneous fission should increase due to the strong hindrance of SF caused by unpaired nucleons. For such nuclei, such as isotopes of elements 113 and 115, one might expect longer consecutive  $\alpha$ -decay chains terminated by the SF of relatively light descendant nuclides with  $Z \leq 105$  [3].

The decay pattern of odd- $Z$  nuclei with larger neutron excess is of interest for nuclear theory. According to microscopic models, the increased stability of superheavy nuclei is determined by spherical proton and neutron shells at  $Z = 114$  (or 120) and  $N = 184$ . In the course of a series of  $\alpha$  decays, the influence of these shells should gradually become weaker for descendant isotopes with smaller proton and neutron numbers. However, the nuclei at the ends of the decay chains are located near the deformed shells at  $Z = 108$  and  $N = 162$ , and their stability against decay by SF should again increase. The observation of nuclei passing from spherical to deformed shapes in the course of their consecutive  $\alpha$  decays could provide valuable information about the influence of significant nuclear structure changes (calculated by theory) on the decay properties of these nuclei (measured in the experiment). For these investigations, we chose the fusion-evaporation reaction  $^{243}\text{Am} + ^{48}\text{Ca}$ , which leads to isotopes of element 115.

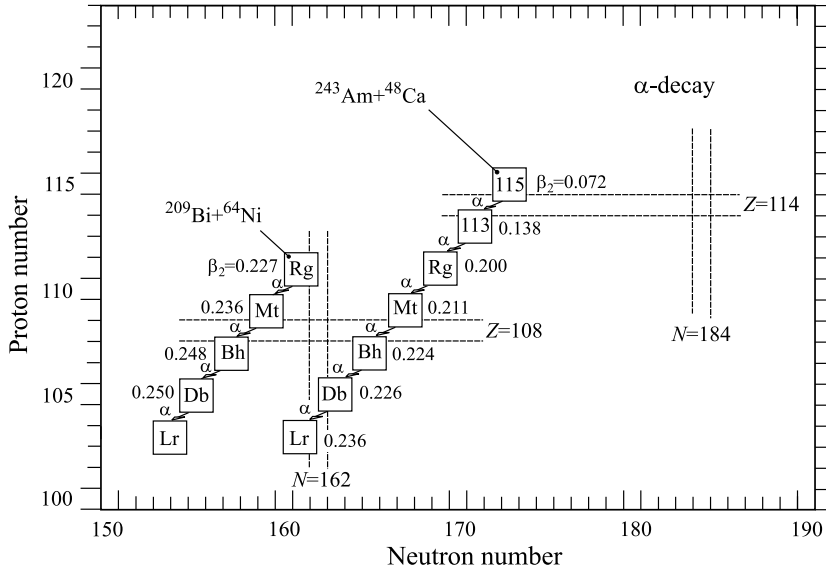


FIG. 1. Expected decay chain for  $^{288}115$  [3] and the decay chain observed for the parent nucleus  $^{272}\text{Rg}$  [8–10]. Calculated deformation parameters  $\beta_2$  [6,7] are shown for each isotope.

Based on the experimental production cross sections  $\sigma_{xn}(E^*)$  of evaporation residues (ERs) measured at different excitation energies of the compound nucleus  $E^* = 35\text{--}53$  MeV in the  $^{244}\text{Pu}(^{48}\text{Ca}, 3\text{--}5n)^{287\text{--}289}114$  reaction [2] and later in the other reactions  $^{242}\text{Pu}(^{48}\text{Ca}, 2\text{--}4n)^{286\text{--}288}114$ ,  $^{238}\text{U}(^{48}\text{Ca}, 3\text{--}4n)^{282,283}112$ , and  $^{248}\text{Cm}(^{48}\text{Ca}, 3\text{--}4n)^{292,293}116$  [2], one can estimate the cross sections for the production of element 115 isotopes in the  $^{243}\text{Am} + ^{48}\text{Ca}$  reaction. According to calculations [2,4,5], the  $3n$ - and  $4n$ -evaporation channels leading to isotopes  $^{288}115$  ( $N = 173$ ) and  $^{287}115$  ( $N = 172$ ) should be observed with the highest yields ( $\sigma_{3n} \approx 3$  pb at  $E^* = 40$  MeV;  $\sigma_{4n} \approx 2$  pb at  $E^* = 42$  MeV).

The  $3n$ -evaporation channel results in the odd-odd isotope of element 115 with mass 288. The expected decay chain of this isotope according to macroscopic-microscopic (MM) calculations [6,7] is shown in Fig. 1. The decay chain of the odd-odd isotope of element Rg ( $Z = 111$ ) with mass 272 produced in the cold fusion reaction  $^{209}\text{Bi}(^{64}\text{Ni}, 1n)^{272}\text{Rg}$  [8–10] is shown for comparison. For the first five  $\alpha$  transitions in the decay chain of  $^{288}115$  with  $\alpha$ -decay energies varying from  $Q_\alpha = 10.95$  MeV for  $^{288}115$  [6] to  $Q_\alpha = 9.08$  MeV for  $^{272}\text{Bh}$  [7], one would only expect a total decay time of 10 s; the probability of spontaneous fission for these isotopes is rather low (taking into account the decay properties of neighboring even- $Z$  nuclei [1,2] and the hindrance against fission of odd isotopes).

We expect a considerable increase in lifetime for the next nuclei,  $^{268}\text{Db}$  ( $Q_\alpha = 7.80$  MeV,  $T_\alpha \geq 5$  h) and  $^{264}\text{Lr}$  ( $Q_\alpha = 6.84$  MeV,  $T_\alpha \geq 100$  d) [7]. For these nuclei, the competition of spontaneous fission or electron capture (EC) with  $\alpha$  decay could be larger. The electron capture of odd-odd isotopes  $^{268}\text{Db}$  or  $^{264}\text{Lr}$  leads to the even-even isotopes  $^{268}\text{Rf}$  or  $^{264}\text{No}$ ; for these isotopes, spontaneous fission with a short lifetime is expected (e.g.,  $T_{\text{SF}} = 1.4$  s is predicted for  $^{268}\text{Rf}$  [11]). Thus, the decay chain of the parent nucleus  $^{288}115$  should be terminated by spontaneous fission after a time interval essentially exceeding the total decay time for all preceding  $\alpha$  decays. A comparable decay pattern is expected for the neighboring isotope  $^{287}115$ .

In our experiments,  $\alpha$ -decay properties proposed by the MM nuclear model [6,7] were used for setting the initial experimental parameters. One should note that the predictions of other models within the Skyrme-Hartree-Fock-Bogoliubov (SHFB) and the relativistic mean-field (RMF) approaches compare well with the MM results (see, e.g., [12,13]). Unfortunately, calculations of the probability of spontaneous fission and electron capture for odd nuclei are rather scarce.

The on-line experiments for the synthesis of element 115 isotopes and their daughters, isotopes of element 113, produced via the  $^{243}\text{Am} + ^{48}\text{Ca}$  reaction were performed with the Dubna gas-filled recoil separator (DGFRS) from July to August, 2003; the results were presented concisely as a Rapid Communication [3]. An off-line chemical experiment aimed at the identification of the spontaneously fissioning isotope  $^{268}\text{Db}$  ( $T_{1/2} \approx 1$  d), observed in [3] following five consecutive  $\alpha$  decays starting with the parent isotope  $^{288}115$ , was proposed [14] and carried out [15,16] in June, 2004. Here, in more detail, we describe both experiments, performed independently, and present their results, which corroborate each other.

## II. EXPERIMENTS WITH THE RECOIL SEPARATOR

The target consisted of the enriched isotope  $^{243}\text{Am}$  (99.9%) deposited as  $\text{AmO}_2$  onto  $1.5\text{-}\mu\text{m}$  Ti foils to a thickness of  $0.36\text{ mg/cm}^2$  of  $^{243}\text{Am}$ ; the foils were covered by a C layer ( $35\text{ }\mu\text{g/cm}^2$ ). Each of six targets had an area of  $5.3\text{ cm}^2$  in the shape of an arc segment with an angular extension of  $60^\circ$  and an average radius of 60 mm. The segments were mounted on a disk that was rotated at 2000 rpm perpendicular to the beam direction. Evaporation products from the complete-fusion reaction  $^{243}\text{Am} + ^{48}\text{Ca}$  recoil out of the target layer and move in the direction of the incident beam particles according to conservation of momentum. The evaporation residues recoiling from the target were separated in flight from beam particles, scattered ions, and various transfer-reaction products by DGFRS [17] (Fig. 2) and were implanted in detectors [18] mounted at the focal plane of the separator at a distance of

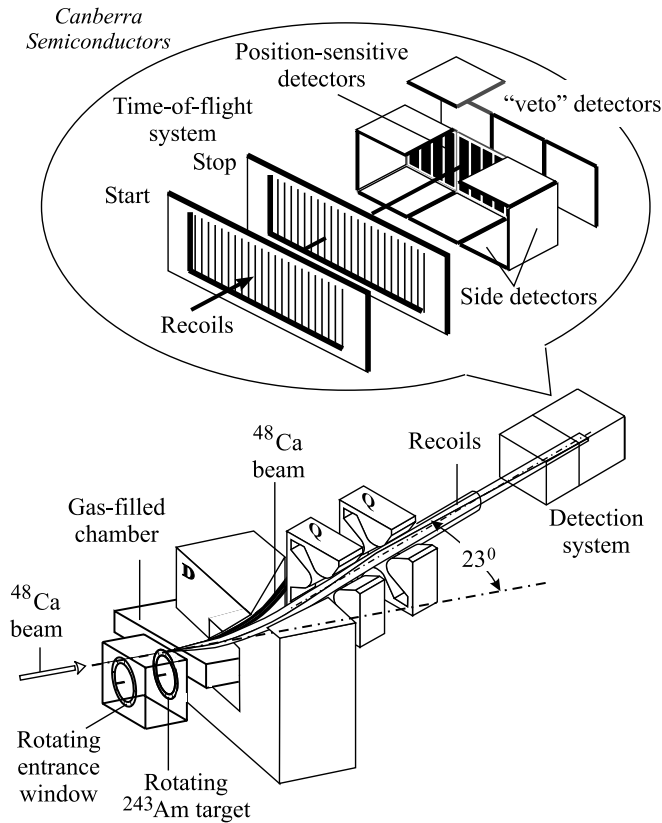


FIG. 2. Schematic view of the Dubna gas-filled recoil separator. D is the dipole magnet and Q is the quadrupole doublet.

about 4m from the target, after a flight time of approximately 1  $\mu$ s. The transmission efficiency of the separator for  $Z = 115$  nuclei is about 35% [17] whereas full-energy  $^{48}\text{Ca}$  projectiles, projectile-like ions, and target-like nuclei are suppressed by factors of  $10^{17}$ ,  $6 \times 10^{14}$ , and  $10^4$ – $10^6$ , respectively.

The experiments were performed at two projectile energies,  $E_{\text{lab}} = 248$  MeV and  $E_{\text{lab}} = 253$  MeV, in the middle of the target layer. At 248 MeV, the evaporation residues are produced with an average kinetic energy of 40 MeV; because of energy losses in the  $\text{AmO}_2$  layer and hydrogen gas (at a pressure of 1 Torr), the average ER energy is reduced to 35 MeV in the center of the dipole magnet. The calculated equilibrium ion charge in hydrogen of 35-MeV ERs is +6.2 (taking into account the results for  $Z = 114$  and 116 ERs [1,2,19]), which corresponds to a magnetic rigidity ( $B\rho$ ) of 2.43 Tm for the mean trajectory in the DGFRS. With a dispersion of 7.5 mm/%  $B\rho$ , an acceptance interval ( $\Delta B\rho$ ) of  $\pm 0.19$  Tm is determined by the horizontal size of the focal-plane detector of 120 mm [17]. Therefore, the magnetic rigidity interval  $B\rho = 2.43 \pm 0.19$  Tm is optimal for the transmission of  $Z = 115$  ERs; other reaction products with rigidities outside this interval should miss the focal-plane detectors. An increase in projectile energy of 5 MeV ( $E_{\text{lab}} = 253$  MeV) results in an increase of initial ER kinetic energy by 1 MeV (0.7 MeV in the center of the dipole magnet) and an increase of the average ( $Z = 115$ ) ion charge of  $\Delta q \approx 0.08$ ; thus the rigidity of ERs remains practically the same [19].

Evaporation residues passing through the separator were registered by a time-of-flight (TOF) system with a detection efficiency of 99.9% and were implanted in a  $4 \times 12$  cm<sup>2</sup> semiconductor detector array with 12 vertical position-sensitive strips. The detection efficiency of these focal-plane detectors for  $\alpha$  particles emitted from the decays of the implanted nuclei is 52% of  $4\pi$ . To detect escaping  $\alpha$ s, the strip detector was surrounded by eight  $4 \times 4$  cm<sup>2</sup> side detectors without position sensitivity, forming a box open to the front (beam) side. In this geometry, the position-averaged detection efficiency for full-energy  $\alpha$  particles of implanted nuclei increases to 87% of  $4\pi$ .

The detection system was calibrated by registering the recoil nuclei and decays ( $\alpha$  or SF) of known isotopes of No and Th and their descendants produced in the reactions  $^{206}\text{Pb}(^{48}\text{Ca}, 2n)$  and  $^{\text{nat}}\text{Yb}(^{48}\text{Ca}, 3-5n)$ , respectively. The full-width-at-half-maximum (FWHM) energy resolution for  $\alpha$  particles implanted in the focal-plane detector was 60–100 keV, depending on the strip and the position within the strip. The  $\alpha$  particles that escaped the focal-plane detector at different angles and registered in a side detector had an energy resolution of the summed signals (side detector plus residual focal-plane detector) of 140–200 keV. If the energy deposited by an  $\alpha$  particle as it recoiled out of the focal-plane detector was lower than the detection threshold of 1.2 MeV (thus its position was also lost) and was detected only by a side detector, its total energy was estimated as a sum of the energy measured by the side detector and half of the threshold energy ( $\approx 0.6$  MeV) with an uncertainty in determining the total energy increased to  $\pm 0.6$  MeV. The assignment of such  $\alpha$  particles to the observed decay chains was made using the calculated probability of random correlations based on the decay rate in the side detectors associated with actual experimental conditions.

The FWHM position resolutions from the signals of correlated decays of nuclei implanted in the detectors were 0.9–1.9 mm for ER- $\alpha$  signals and 0.5–0.9 mm for ER-SF signals. If an  $\alpha$  particle was detected by both the focal-plane ( $\Delta E_{\alpha 1}$ ) and a side detector ( $\Delta E_{\alpha 2}$ ) (i.e.,  $E_{\alpha} = \Delta E_{\alpha 1} + \Delta E_{\alpha 2}$ ), the position resolution depended on the amplitude  $\Delta E_{\alpha 1}$  (see, e.g., Fig. 4 in [20]) but was generally inferior to that obtained for the full-energy signal.

Fission fragments from the decay of  $^{252}\text{No}$  implants produced in the  $^{206}\text{Pb} + ^{48}\text{Ca}$  reaction were used for the total kinetic energy (TKE) calibration. The measured fragment energies ( $E_{\text{tot}} = E_{F1} + E_{F2}$ ) were not corrected for the pulse-height defect of the detectors, the energy loss in the detectors' entrance windows or dead layers, or the energy loss in the pentane gas filling the detection system (at a pressure of about 1.7 Torr) of the escaping fragment ( $E_{F2}$ ). The mean sum energy loss of fission fragments from the SF decay of  $^{252}\text{No}$  was about 20 MeV. The TKE of fissioning nuclei with  $Z > 102$  was determined as the sum  $E_{\text{tot}} + 20$  MeV. The systematic uncertainty in estimating the TKE value is 5 MeV when both fission fragments were detected.

From model calculations and the available experimental data for neighboring even- $Z$  nuclei, one can estimate the expected  $\alpha$ -particle energies for the isotopes of element 115 and their descendant nuclei that could be produced in the

$^{243}\text{Am} + ^{48}\text{Ca}$  reaction. This allowed us to employ a special low-background detection scheme for the nuclides to be investigated [1,2,18]. In the bombardment of  $^{243}\text{Am}$ , the beam was switched off after a recoil signal was detected with parameters of implantation energy and TOF expected for  $Z = 115$  evaporation residues, followed by an  $\alpha$ -like signal with an energy of  $9.6 \leq E_\alpha \leq 11.0$  MeV, in the same strip, within a 1.4- to 1.9-mm-wide position window and a time interval of up to 8 s. The beam-off interval was initially set at 2 min. In this time interval, if an  $\alpha$  particle with  $E_\alpha > 8.6$  MeV was registered in any position of the same strip, the beam-off interval was automatically extended to 12 min. In the 12-min period, if other  $\alpha$  particles with energies expected for heavy nuclei were observed, we prolonged the beam-off pause up to 2.7 h.

This experimental running condition was a compromise between the inevitable loss of beam dose (10% of the beam time was lost) and the necessity of a beam pause for the registration of long-duration sequential decays of the daughter nuclides with  $Z \leq 113$  under very low background conditions. With the experimentally measured counting rates for random ER- $\alpha_1$  pairs that initiated beam-off conditions and subsequent beam-off  $\alpha$  particles with  $E_\alpha > 8.6$  MeV (mainly  $^{212}\text{Po}$ ; see the following), we could expect only a few 12-min beam interrupts that were not associated with true correlated events. Indeed, during the 27-d duration of the experiment, only two such pauses occurred; one  $\alpha$  particle was observed in each case with  $E_\alpha = 8.72$  and 8.80 MeV but in different positions than the preceding ER- $\alpha_1$  events. Note that the probability of detecting the second random  $\alpha$  particle with  $E_\alpha > 8.6$  MeV in the same strip during the 12-min beam-off interval was 0.02; the probability of registering random  $\alpha$ s in the same position as the preceding ER- $\alpha_1$  pair was only  $5 \times 10^{-5}$  (or  $2 \times 10^{-4}$  for such random chains during the whole experiment).

Using the Monte Carlo random probability method [21],  $10^7$  random artificial events ( $\alpha_{\text{ar}}$ ) were inserted into the data and the probability of observing an in-beam random ER- $\alpha_1$ - $\alpha_2$ - $\alpha_{\text{ar}}$  chain was calculated to be  $1.5 \times 10^{-4}$ . The following conditions were met to arrive at the probabilities calculated: ER energies = 7–13 MeV,  $\alpha_1$  energies = 10–11 MeV,  $\alpha_2$  energies = 9.5–10.5 MeV, position window =  $\pm 2.0$  mm, maximum ER- $\alpha_1$  correlation time = 1 s, and maximum  $\alpha_1$ - $\alpha_2$  and  $\alpha_2$ - $\alpha_{\text{ar}}$  correlation times of 4 and 40 s, respectively. These parameters were specifically chosen as conservative windows around the decays observed in the experiment. Events contributing to the calculated probabilities were not constrained to satisfy the Geiger-Nuttall relationship. Therefore, only one in-beam random ER- $\alpha_1$ - $\alpha_2$ - $\alpha_3$  chain (with  $E_{\alpha_3} = 9.5$ –10.5 MeV; see Fig. 3) might be expected to be observed in the experiment.

### III. EXPERIMENTAL RESULTS

The Coulomb barrier in the  $^{243}\text{Am} + ^{48}\text{Ca}$  reaction is 236 MeV [22]. With 248-MeV  $^{48}\text{Ca}$  projectiles, the excitation energy of the compound nucleus  $^{291}115$  for central collisions is 40 MeV, corresponding to the expected maximum for the  $3n$ -evaporation channel [5], resulting in production of  $^{288}115$  with neutron number  $N = 173$ .

The intensity of the  $^{48}\text{Ca}$ -ion beam accelerated by the U400 cyclotron was 1.3 pμA at the target. Irradiation of the  $^{243}\text{Am}$  target by 248-MeV  $^{48}\text{Ca}$  projectiles was performed between July 14 and 29, 2003 [3]. During the 270-h run, a beam dose of  $4.3 \times 10^{18}$  projectiles was delivered to the target. The systematic uncertainty in the beam energy was 1 MeV. With the energy spread of the incident cyclotron beam, the small variation of the beam energy during irradiation, and the energy losses in the target ( $\approx 3.3$  MeV), we expected the resulting compound nuclei  $^{291}115$  to have excitation energies between 38.0 and 42.3 MeV. Excitation energies of the compound nuclei are calculated using the masses of [23]. The beam energy losses in the separator's entrance window (1.5-μm Ti foil), hydrogen fill gas ( $5.3 \mu\text{g}/\text{cm}^2$ ), target backing, and target layer were calculated using the data of Hubert *et al.* for solid materials [24] and Northcliffe and Schilling for gases [25].

In this  $^{243}\text{Am} + ^{48}\text{Ca}$  experiment, we had 577 short-duration beam interrupts, each lasting 2 min. There were three other cases with longer beam pauses associated with the decay chains shown in Table I.

In the first decay chain, implantation of a 10.4-MeV recoil in the center of strip 2 (at 18.5 mm from the top of the strip) of the focal-plane detector was followed 80.3 ms later by an  $\alpha$  particle with  $E_\alpha = 10.51$  MeV and a position of 18.6 mm. Detection of this sequence caused the beam to switch off, and four more  $\alpha$  decays were detected over a total time interval of 29 s in the absence of a beam-associated background. The second  $\alpha$  particle was detected with energies  $\Delta E_{\alpha 1} = 2.01$  MeV and  $\Delta E_{\alpha 2} = 8.03$  MeV by both the focal-plane and side detectors ( $E_\alpha = 10.04$  MeV), 0.376 s later. Then, in another 3.146 s, the third  $\alpha$  particle with  $E_\alpha = 9.72$  MeV, and 1.055 s later the fourth  $\alpha$  particle with  $E_\alpha = 9.65$  MeV, were registered by the focal-plane detector. In another 24.103 s, the last  $\alpha$  decay ( $E_\alpha = 9.23 \pm 0.61$  MeV) was registered by the side detector only. During the remainder of the 2.7-h beam-off period following the last  $\alpha$  particle, no  $\alpha$  particles with  $E_\alpha > 7.6$  MeV were registered in strip 2 of the focal-plane detectors, and the beam was switched on. The SF decay of the final nucleus in this chain was detected 28.69 h after the last  $\alpha$  decay by both the focal-plane and side detectors with energies  $E_{F1} = 150$  MeV (this signal corresponds to the total energy of one SF fragment moving deeper into the detector plus part of the energy of the second fragment escaping the focal plane detector) and  $E_{F2} = 55$  MeV (part of the energy of the second fragment registered by the side detector) (and  $E_{\text{tot}} = 205$  MeV). A search was performed to identify ERs and  $\alpha$  decays correlated closely in time ( $< 60$  s) and position with this SF event. No such correlations were found.

During this experiment, two other decay chains were observed that were very similar to the first one (see Table I). The implantations of recoils in strips 3 and 4 of the focal-plane detector were followed by  $\alpha$  particles with  $E_\alpha = 10.38$  and 10.50 MeV. These sequences caused the beam to switch off and four more  $\alpha$  decays in each decay sequence were detected in total time intervals of 15 s and 20 s, respectively. The SF decays of the final nuclei in these chains were detected 23.5 h and 16.8 h, respectively, after the last  $\alpha$  decay. The fifth  $\alpha$  decay in the first chain and second and fourth  $\alpha$  decays in

TABLE I. Time sequences in the decay chains observed at two  $^{48}\text{Ca}$  energies.

		$E_{\text{lab}} = 248 \text{ MeV}$			$E_{\text{lab}} = 253 \text{ MeV}$	
Date		7/24 12:40	7/25 11:39	7/29 10:04		8/08 00:58
Isotope		Strip 2	Strip 3	Strip 4	Isotope	Strip 7
ER(115)	$E_{\text{ER}}$ , MeV	10.4	11.0	9.1	ER(115)	12.2
	$y_{\text{ER}}$ , mm	18.5	23.3	18.8		18.0
$^{288}\text{115}$	$\delta t_{\text{ER}-\alpha 1}$ , ms	80.3	18.6	279.8		46.6
	$E_{\alpha 1}$ , MeV	10.51	10.38	10.50	$^{287}\text{115}$	10.59
	$y_{\alpha 1}$ , mm	18.6	23.7	18.5		17.6
$^{284}\text{113}$	$\delta t_{\alpha 1-\alpha 2}$ , s	0.3757	1.196	0.5172		0.1474
	$E_{\alpha 2}$ , MeV	10.04 <sup>a</sup>	9.48 <sup>b</sup>	10.00	$^{283}\text{113}$	10.12
	$y_{\alpha 2}$ , mm	21.3	—	18.7		17.6
$^{280}\text{Rg}$	$\delta t_{\alpha 2-\alpha 3}$ , s	3.146	10.599	1.793		0.2450
	$E_{\alpha 3}$ , MeV	9.72	9.76	9.76	$^{279}\text{Rg}$	10.37 <sup>a</sup>
	$y_{\alpha 3}$ , mm	18.4	23.7	18.1		—
$^{276}\text{Mt}$	$\delta t_{\alpha 3-\alpha 4}$ , s	1.055	0.2487	1.834		0.0140
	$E_{\alpha 4}$ , MeV	9.65	9.80 <sup>b</sup>	9.74	$^{275}\text{Mt}$	10.33
	$y_{\alpha 4}$ , mm	18.8	—	19.2		17.7
$^{272}\text{Bh}$	$\delta t_{\alpha 4-\alpha 5}$ , s	24.103	2.964	15.388		
	$E_{\alpha 5}$ , MeV	9.23 <sup>b</sup>	9.02	8.97 <sup>a</sup>	$^{271}\text{Bh}$	—
	$y_{\alpha 5}$ , mm	—	23.6	18.1		
$^{268}\text{Db}$	$\delta t_{\alpha 5-\text{SF}}$ , h	28.69	23.54	16.80		1.766
	$E_{\text{SF}}$ , MeV	205 <sup>c</sup>	200 <sup>c</sup>	140	$^{267}\text{Db}$	206 <sup>c</sup>
	$y_{\text{SF}}$ , mm	18.2	23.2	17.8		17.9

<sup>a</sup> $\alpha$  particles with  $E_{\alpha} = 10.04, 8.97$ , and  $10.37$  MeV were detected by both the focal-plane and side detectors with energies of  $2.01 + 8.03$ ,  $3.14 + 5.83$  and  $1.30 + 9.03$  MeV, respectively.

<sup>b</sup>Energies of events detected by side detectors only.

<sup>c</sup>SF events with  $E_{\text{SF}} = 205, 200$ , and  $206$  MeV were detected by both the focal-plane and side detectors with energies  $E_{\text{tot}} = 150 + 55$ ,  $148 + 52$ , and  $170 + 36$  MeV, respectively.

the second chain were registered by the side detectors only. The energies deposited by these  $\alpha$  particles in the focal-plane detector as well as their position signals were not registered. However, given the  $\alpha$ -counting rates in the side detectors, the probability that these  $\alpha$  particles appeared in the detector during a given 30-s time interval as random events is estimated to be only 1.5% [26,27], so we assign them to the decay of the same implanted nuclei.

Estimation of the probability of the random appearance of the signals in the observed decay chains, in particular five  $\alpha$  particles during 15–30 s and a subsequent spontaneous fission following a time interval of about 1d can be determined from the spectra of events accumulated over the entire 270-h experiment. The spectrum of  $\alpha$ -like signals (all events without a TOF signal) in all of the strips in the energy range of  $7 \leq E_{\alpha} \leq 11$  MeV is shown in Fig. 3 (top panel). In this figure, we also show the  $\alpha$ -particle spectrum detected in beam-off time intervals (see the preceding discussion). In the beam-off  $\alpha$ -particle spectrum we mainly observed the peaks originating from isotopes of Po, the decay products of the long-lived isotopes of Ra-Th produced in transfer reactions, and  $^{211}\text{Po}$ , the descendant nucleus of  $^{219}\text{Th}$  produced in calibration experiments with a  $^{\text{nat}}\text{Yb}$  target. The total counting rate for  $\alpha$  particles with  $E_{\alpha} > 8.9$  MeV by the whole detector array

during beam-off pauses (including those shown in Table I) was  $0.7 \text{ h}^{-1}$ . The majority of the events with  $E_{\alpha} = 8.0$ – $9.5$  MeV result from  $\alpha$  decays of the short-lived descendants  $^{212}\text{Po}$  ( $T_{1/2} = 0.3 \mu\text{s}$ ,  $E_{\alpha} = 8.78$  MeV) and  $^{213}\text{Po}$  ( $T_{1/2} = 4.2 \mu\text{s}$ ,  $E_{\alpha} = 8.38$  MeV) [28] detected in coincidence with  $\beta^{-}$  decays of the precursors  $^{212}\text{Bi}$  and  $^{213}\text{Bi}$  (see, e.g. [1]). Note that in the high-energy part of the  $\alpha$ -particle spectrum ( $E_{\alpha} \geq 9.5$  MeV) only eight events were detected, seven of which (marked black), as we will demonstrate in the following, belong to the decay chains of  $^{288}\text{115}$ .

Switching the beam off essentially eliminates the background above 9 MeV (see Fig. 3), where four  $\alpha$  decays were observed in each chain (see Table I). The probability that any one of the four  $\alpha$  particles observed during a 30-s interval is due to random detector background is  $6 \times 10^{-3}$ , without taking into account the correlation in position and strip number for the subsequent events. Applying both of these factors will further reduce this probability by more than two orders of magnitude.

Comparing beam-off with beam-on events, one can determine the probability of the random appearance of the first correlated pair of ER- $\alpha_1$  signals that caused the beam to be switched off. The total spectrum of  $\alpha$ -like particles that caused the beam to be switched off in both series of experiments is shown in Fig. 4. Here, the solid histogram shows the energies

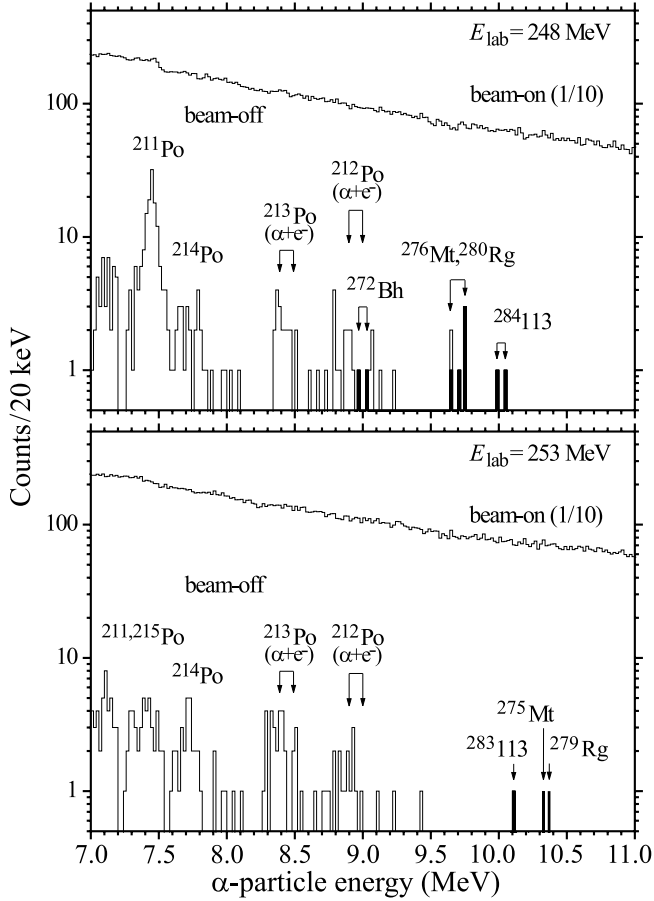


FIG. 3. Total beam-on  $\alpha$ -like signal and beam-off  $\alpha$ -particle energy spectra of events registered by the focal-plane detector and by both the focal-plane and side detectors in the reaction  $^{243}\text{Am} + ^{48}\text{Ca}$  at two projectile energies. The solid histogram shows the energies of events observed during beam-off periods in the correlated decay chains (see Table I).

of events that caused the beam to be switched off and that were followed by two or more beam-off  $\alpha$  particles with  $E_\alpha = 8.5\text{--}11$  MeV, without taking into account the position and strip number for the subsequent events. As will be shown in the following, all of these  $\alpha$  particles belong to the decays of  $^{287}115$  and  $^{288}115$ . Thus, the probability that each of the ER- $\alpha_1$  events followed by a subsequent  $\alpha_2\text{--}\alpha_5$ -SF decay chain randomly caused the beam to be switched off is  $10^{-5}$ .

The total spectrum of high-energy signals with  $E \geq 40$  MeV (without an associated TOF signal) is presented in Fig. 5 (top panel). In cases where fission signals were registered by both the focal-plane and the side detectors, the sum energy is given. The background signals (scattered  $^{48}\text{Ca}$  ions, fragments of the induced fission of the target, etc.) appear in the energy range  $E \leq 120$  MeV; they are not observed in the beam-off spectrum. The signals of SF fragments arising from the decays of heavy nuclei are expected at higher energies, with  $E \geq 130$  MeV [1,2].

In the experiment with 248-MeV  $^{48}\text{Ca}$  ions, we observed only seven SF events with  $E_F \geq 130$  MeV (Fig. 5). In addition to the three previously mentioned events, three other SF

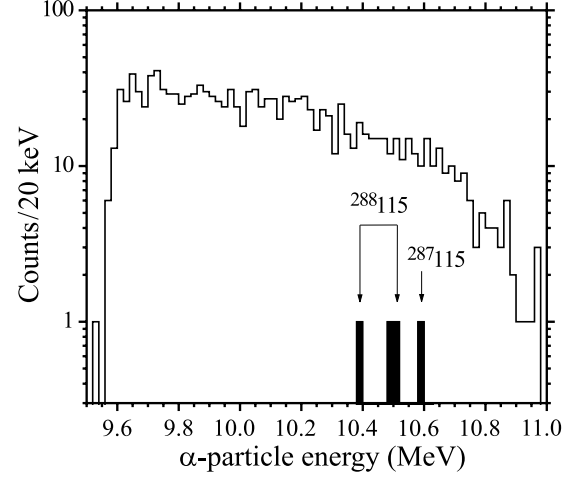


FIG. 4. Total energy spectrum of  $\alpha$ -like events that stopped the beam during the  $^{243}\text{Am} + ^{48}\text{Ca}$  experiment. The solid histogram shows the energies of  $\alpha$  particles that switched off the beam and were followed by two or more beam-off  $\alpha$  particles with  $E_\alpha = 8.5\text{--}11$  MeV.

events with measured energies of 147, 168, and 154 MeV were detected 0.51 ms, 4.1 ms, and 2.07 ms after the implantation of corresponding recoil nuclei in strips 12, 10, and 11, respectively. For the second and third event, both the focal-plane and side detectors registered fission fragments. Based on the apparent lifetime, we assign these events to the spontaneous fission of the 0.9-ms  $^{244\text{mf}}\text{Am}$  isomer, a product of transfer reactions with the  $^{243}\text{Am}$  target [28]. The DGFRS suppresses the yield of such products by a factor of  $10^5$  [1,17]. For one event with  $E_{\text{tot}} = 146$  MeV, no appropriate ER-SF correlation was found. However, before the  $^{243}\text{Am} + ^{48}\text{Ca}$  experiment, during a 390-h off-line background measurement, we detected three SF decays of long-lived nuclei [e.g.,  $^{252}\text{Cf}$

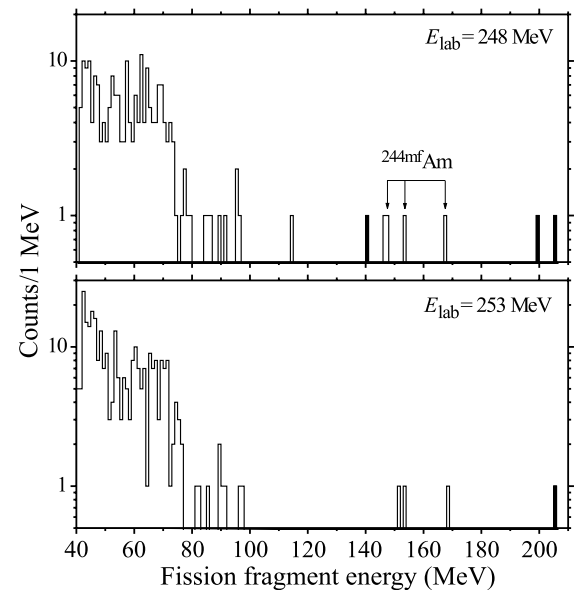


FIG. 5. Total fission-fragment energy spectra; the solid histogram shows the energies of events observed in the correlated decay chains.

( $T_{1/2} = 2.65$  yr)], produced in incomplete fusion reactions in the previous experiments [2,20] where the same set of detectors was used. Thus, the registration of one more SF event ( $E_{\text{tot}} = 146$  MeV, strip 2) from the decay of long-lived nuclei corresponds to the background level of Cf isotopes and was to be expected.

The three SF events that were observed in the strips and positions corresponding to the three ER- $\alpha_1$ -...- $\alpha_5$  decay chains were registered with high TKEs of  $E_{\text{tot}} = 205$  MeV ( $150 + 55$  MeV), 200 MeV ( $148 + 52$  MeV), and  $E_{F1} = 140$  MeV (with only the focal-plane detector registering a fission fragment). When we take into account the various sources of energy losses by the SF fragments in the pentane gas and detector, the total kinetic energy of these SF events is 225 MeV. The probability that these SF events appeared in the detector as random events and are not the members of the three preceding ER- $\alpha_1$ -...- $\alpha_5$  decay chains is less than  $10^{-7}$ .

The position deviations of the detected signals of recoil nuclei and subsequent sequential decays ( $\alpha$  and SF) for all three decay chains observed in this experiment and the chain registered at higher projectile energy (see the following) are shown in Fig. 6(a); they indicate a strong position correlation among the observed decays.

The ER- $\alpha_1$ - $\alpha_2$ - $\alpha_3$ - $\alpha_4$ - $\alpha_5$  sequences were detected in total time intervals of 15–29 s; the SF decays of the final nuclei in these chains were detected 17–29 h after the last  $\alpha$  decay. As seen in Table I, the  $\alpha$ -particle energies for each isotope in all decay chains are equivalent within the energy resolutions of the detectors. The similarity of decay times for the three independent measurements of each nuclide arising from decays of  $^{288}\text{115}$  is presented in Fig. 6(b). In the figure, the decay time associated with each measurement is scaled to the average decay constant for the three measurements. This allows us to characterize each decay type by a single half-life value, bearing in mind the expected statistical distribution of values, indicated in the figure by the smooth curve. Therefore, one can conclude that in all three cases we observed decay chains originating from the same parent nucleus. It is most reasonable that the observed decay chains originate from the isotope  $^{288}\text{115}$ , produced in the complete fusion reaction  $^{243}\text{Am} + ^{48}\text{Ca}$  followed by evaporation of three neutrons from the compound nucleus  $^{291}\text{115}$ . The corresponding cross section for the  $3n$ -evaporation channel at 248-MeV  $^{48}\text{Ca}$ -ion energy is  $\sigma_{3n} = 2.7^{+4.8}_{-1.6}$  pb.

We can support this conclusion through the application of the systematic behavior of the cross sections  $\sigma_{xn}(E^*)$  of complete-fusion reactions. Indeed, if the  $3n$ -evaporation channel was observed at  $E^* = 40$  MeV, then a small increase of the bombarding energy (by about 5 MeV or 2%) should result in decreasing the production cross section by a factor of several times. That is why the next experiment was performed at the  $^{48}\text{Ca}$  energy  $E_{\text{lab}} = 253$  MeV. This resulted in an excitation energy of the compound nucleus  $^{291}\text{115}$  spanning 42.4–46.5 MeV, close to the expected maximum for the cross section of the  $4n$ -evaporation channel [5].

The second experiment was performed between July 29 and August 10, 2003 [3]. During the 250-h run, the same beam dose of  $4.3 \times 10^{18}$   $^{48}\text{Ca}$  projectiles was delivered to the target as in the previous experiment.

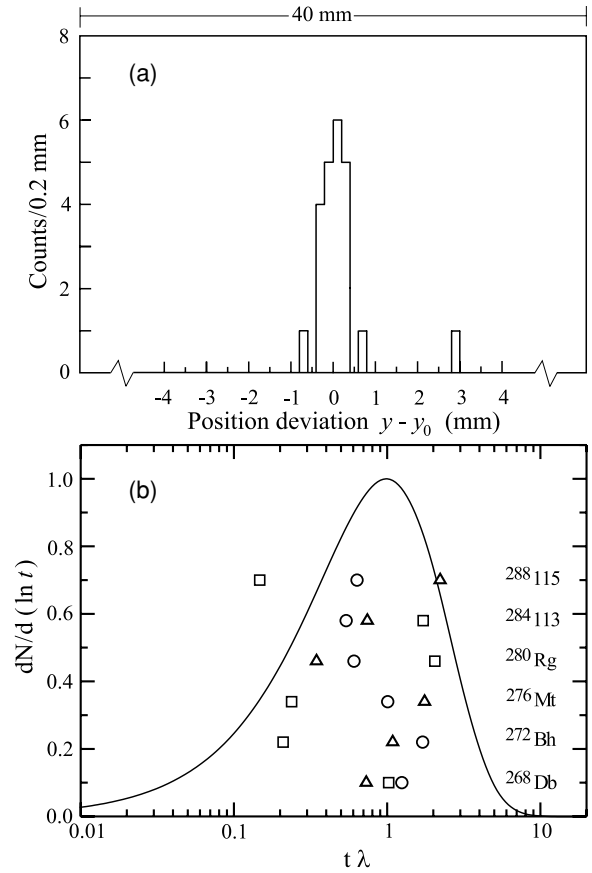


FIG. 6. (a) Position deviations of all signals (ERs,  $\alpha$  particles, and SF fragments) in the observed decay chains. The position of one  $\alpha$  particle deviates from the average value by more than 1 mm, caused by the low energy,  $\Delta E_{\alpha 1} = 2.0$  MeV, deposited in the focal-plane detector resulting in degraded position resolution. (b) Relative time intervals of all events in the observed decay chains originating from  $^{288}\text{115}$  ( $\lambda = \ln 2/T_{1/2}$ ) compared with the average half-lives assigned to the appropriate nuclides. Circles, squares, and triangles correspond to the first ( $\circ$ ), second ( $\square$ ), and third ( $\triangle$ ) decay chains shown in Table I, respectively.

In this  $^{243}\text{Am} + ^{48}\text{Ca}$  experiment, we had 755 beam interrupts lasting a total of about 27 h. One decay chain only, consisting of four  $\alpha$  decays and a spontaneous fission, was registered at  $E_{\text{lab}} = 253$  MeV (see Table I). The beam was switched off after the detection of an ER signal followed 46.6 ms later by an  $\alpha$  particle with  $E_{\alpha} = 10.59$  MeV in the same position ( $\Delta y_{\text{ER}-\alpha 1} = 0.4$  mm) in strip 7 (see Fig. 4). Three other  $\alpha$  decays were detected in a time interval of 0.4 s in the absence of beam-associated background (Fig. 3). The first of them ( $E_{\alpha 2} = 10.12$  MeV) was registered in 0.147 s; after another 0.245 s, the next  $\alpha$  particle with  $E_{\alpha 3} = 10.37$  MeV ( $1.30 + 9.07$  MeV) was detected by both the focal-plane and a side detector; the last  $\alpha$  particle ( $E_{\alpha 4} = 10.33$  MeV) was observed 14.0 ms later. After 106 min, the terminal SF event was detected in-beam with a sum energy of 206 MeV ( $E_{\text{tot}} = 170 + 36$  MeV) in the same position ( $\Delta y_{\text{ER-SF}} = 0.1$  mm) in strip 7.

At 253 MeV, the random counting rates were practically the same as in the previous experiment (see Figs. 3 and 5).

The probability that the terminal SF event is not a member of the preceding ER- $\alpha_1$ -...- $\alpha_4$  decay chain is less than  $10^{-4}$ . In addition to this SF event with  $E_{\text{tot}} = 206$  MeV, only three long-lived background SF nuclei, with measured fission-fragment energies of 168, 154, and 151 MeV, were observed in strips 4, 3, and 1, respectively (see Fig. 5).

As can be seen in Table I, the decay pattern of these nuclei is similar to those in the previous three chains observed at  $E_{\text{lab}} = 248$  MeV. However, the decay properties are significantly different. The total decay time of this chain is 10 times shorter, and the  $\alpha$  decays are distinguished by higher  $\alpha$ -particle energies and shorter lifetimes; in particular, the  $\alpha$ -particle energies of the third and fourth nuclei in the last chain are larger by 0.6 MeV. Thus, the short-lived decay chain originates from another parent nucleus.

The aforementioned ER- $\alpha_1$ -...- $\alpha_5$ -SF decay chains observed at  $E^* = 40$  MeV, corresponding to the expected maximum yield of the  $3n$ -evaporation channel, were not observed at  $E^* = 44$  MeV. This is in agreement with expectations for the  $3n$  channel. Consistent with this observation, the shorter lived decay chain was not observed at  $E^* = 40$  MeV. It is reasonable that the shorter lived decay chain originates from the odd-even isotope  $^{287}\text{115}$ , produced in the reaction  $^{243}\text{Am}(^{48}\text{Ca}, 4n)$  at the higher excitation energy,  $E^* = 44$  MeV. The corresponding cross section for the  $4n$ -evaporation channel is  $\sigma_{4n} = 0.9^{+3.2}_{-0.8}$  pb.

In the single decay chain originating from  $^{287}\text{115}$ , we propose that we have missed the  $\alpha$  decay of  $^{271}\text{Bh}$ . Indeed, in the decay chains shown in Table I, 19  $\alpha$  particles were registered in all, using a detector with 87% efficiency, so the loss of one  $\alpha$  particle seems rather probable. Because of the large energies and relatively long decay times of the four observed  $\alpha$  particles, they could not be assigned to the decays of nuclei with  $Z \leq 107$  (see the following). The expected  $T_\alpha$  value for  $^{271}\text{Bh}$  should be  $\sim 10$  s ( $Q_\alpha = 9.07$  MeV [7],  $T_\alpha \approx 5$  s for an allowed transition), which is much shorter than the interval between the last observed  $\alpha$  particle and the terminating SF event but is much longer than the intervals between the observed correlated  $\alpha$  particles. The assignment of SF to  $^{271}\text{Bh}$  would result in a  $Q_\alpha$  upper limit for this isotope 0.7 MeV lower than the calculated value [7] (applying a hindrance factor of 5). So, we suggest that an unobserved  $\alpha$  decay of  $^{271}\text{Bh}$  occurred in the time interval between the fourth  $\alpha$  particle and the spontaneous fission.

As in the first experiment, a search was performed to identify  $\alpha$  particles with  $E_\alpha > 7.0$  MeV correlated in position to the observed  $\alpha$  decays. No correlated  $\alpha$  particles were observed within an hour after the last  $\alpha$  decay. The experimental decay scheme for  $^{287}\text{115}$  is also supported by the agreement of the observed decay properties of the other nuclides in the decay chain with the expectations of theory (see the following). This means that the SF occurs directly in the decay of  $^{267}\text{Db}$  since the calculated  $\alpha$ -decay and EC-decay energies for this isotope are rather low ( $Q_\alpha = 7.41$  MeV [7],  $T_\alpha \sim 10$  d;  $Q_{\text{EC}} = 0.79$  MeV [29],  $T_{\text{EC}} \sim 1$  d [30]) and their expected partial half-lives significantly exceed the observed time interval of 106 min.

We have discussed the decay properties of the new nuclei. The initial events (with a TOF signal) in the observed ER- $\alpha_1$ -...- $\alpha_5$ -SF chains provide information about recoiling nuclei with  $Z = 115$ . The distribution of the four observed decay chains over the strips is a consequence of the magnetic rigidity of the recoils in the gas-filled separator. Based on the results of previous experiments [1,19], the magnetic rigidity of the separator was set for observation of such ERs in the center of the focal-plane detector. In fact, the isotopes of element 115 were observed in strips 2, 3, 4, and 7 of the 12-strip focal plane detector. The observed deflection corresponds to the separation of  $Z = 115$  recoils traversing the hydrogen media with an average ion charge of  $6.25 \pm 0.30$ , an intermediate value between recently measured ion charges of nuclei with  $Z = 114$  and  $116$  [1,2,19]. The mean observed energies of the recoils,  $E_{\text{ER}} = 10.7$  MeV, also agree well with those measured previously ( $E_{\text{ER}} = 11.1 \pm 2.1$  MeV) in our  $^{242,244}\text{Pu} + ^{48}\text{Ca}$  and  $^{245,248}\text{Cm} + ^{48}\text{Ca}$  experiments [1,2].

The cross section values of the  $^{243}\text{Am}(^{48}\text{Ca}, 3-4n)^{287,288}\text{115}$  reaction measured at two  $^{48}\text{Ca}$  energies are comparable with results of recent experiments [2] where excitation functions for the reactions of  $^{238}\text{U}$ ,  $^{242}\text{Pu}$ ,  $^{244}\text{Pu}$ , and  $^{248}\text{Cm}$  with  $^{48}\text{Ca}$  have been measured (see Table II). Comparing the decay properties of the observed nuclei (Table I) and their production cross sections, we can deduce a consistent picture for the atomic numbers of the observed nuclides.

We do not consider other reaction channels accompanied by emission of light charged particles, (e.g.,  $pxn$  or  $\alpha xn$ ) because of their lower probability in comparison with  $xn$ -evaporation channels. These channels were not observed in either cold or hot fusion reactions induced by projectiles with  $A > 40$

TABLE II. Cross sections of the  $xn$ -evaporation channels for the given reactions.

Reaction	$Z_{\text{CN}}/A_{\text{CN}}$	Cross section (pb)			
		$\sigma_{2n}$	$\sigma_{3n}$	$\sigma_{4n}$	$\sigma_{5n}$
$^{238}\text{U} + ^{48}\text{Ca}$	112/286		$2.5^{+1.8}_{-1.1}$	$0.6^{+1.6}_{-0.5}$	
$^{242}\text{Pu} + ^{48}\text{Ca}$	114/290	$0.5^{+1.4}_{-0.4}$	$3.6^{+3.7}_{-1.7}$	$4.5^{+3.6}_{-1.9}$	
$^{244}\text{Pu} + ^{48}\text{Ca}$	114/292		$1.7^{+2.5}_{-1.1}$	$5.3^{+3.6}_{-2.1}$	$1.1^{+2.6}_{-0.9}$
$^{243}\text{Am} + ^{48}\text{Ca}$	115/291		$3.7^{+1.3a}_{-1.0}$	$0.9^{+3.2}_{-0.8}$	
$^{248}\text{Cm} + ^{48}\text{Ca}$	116/296		$1.2^{+1.8}_{-0.8}$	$3.3^{+2.5}_{-1.4}$	

<sup>a</sup>Average value determined from DGFRS and chemistry experiments.



leading to heavy nuclei in numerous previous experiments (see, e.g. [2,8–10,31–35]). As will be shown in the following these channels were excluded by direct and independent identification of the atomic numbers of nuclei in the ER- $\alpha_1$  . . . - $\alpha_5$ -SF decay chains in the chemistry experiment.

#### IV. OFF-LINE CHEMICAL SEPARATION OF SF NUCLEI WITH $Z = 105$

From the analysis of the gas-filled separator experimental data, one can conclude that in the  $3n$ - and  $4n$ -evaporation channels of the reaction  $^{243}\text{Am} + ^{48}\text{Ca}$  we observed two isotopes of element 115,  $^{287}\text{115}$  and  $^{288}\text{115}$ , which underwent five consecutive  $\alpha$  decays and were terminated by SF nuclides. As expected, the longer lived ER- $\alpha_1$  . . . - $\alpha_5$ -SF decay chains in which the half-life of the final nucleus was  $T_{\text{SF}} = 16^{+19}_{-6}$  h were associated with the  $3n$ -reaction channel, arising from the decay of the odd-odd isotope  $^{288}\text{115}$ . Since all of the consecutive  $\alpha$  decays and the SF are strongly correlated with each other and the order of occurrence of the nuclei in the decay chains has been determined, then *the identification of the atomic number of any nucleus in this chain would independently prove the synthesis of the previously unknown elements 115 and 113.*

One method for identifying the atomic number of a nucleus is to use classical chemical methods, which were used in the first identification and characterization of many of the artificial elements heavier than uranium (see, e.g., Ref. [36] and references therein). With a half-life of about one day, we are presented with an opportunity to perform a chemistry experiment to determine the atomic number of the final nuclide in the  $^{288}\text{115}$  decay chain,  $^{268}\text{Db}$  ( $Z = 105$ ), thereby independently identifying the other atomic numbers in the decay chain.

According to its atomic configuration in the ground state, Db should belong to group 5 of the Periodic Table as a heavier homologue of Nb and Ta. The chemical behavior of Db has been investigated through the study of 34-s  $^{262}\text{Db}$ . In the processes of extraction by Aliquat 336 [37] from chloride solutions, its behavior is most close to that of Nb and differs from Ta and Pa (pseudo-homologue), whereas in the extraction from fluoride solutions it is analogous to Nb and Ta and differs from Pa. In general, one observes the theoretically predicted inversion of properties within the group of homologues with the transition from 5d to 6d elements (i.e., in its chemical properties Db is more similar to Nb than to Ta [38]).

Taking into account these results, we developed a method of sorption extraction for the group 5 elements as anionic fluoride complexes. Bearing in mind that the  $Z = 105$  isotope of interest undergoes SF, we paid special attention to separating the group 5 elements from the actinides and, most importantly, from spontaneously fissioning isotopes (e.g.,  $^{252}\text{Cf}$  and  $^{254}\text{Cf}$ ).

A diagram of the setup for target irradiation and collection of ERs for chemical studies is shown in Fig. 7. The 32-cm<sup>2</sup> rotating target consisted of the enriched isotope  $^{243}\text{Am}$  (99.9%) in oxide form. The target material was deposited onto 1.5- $\mu\text{m}$  Ti foils to a thickness of 1.2 mg/cm<sup>2</sup> of  $^{243}\text{Am}$ . After leaving the target, the recoiling reaction products were stopped in a

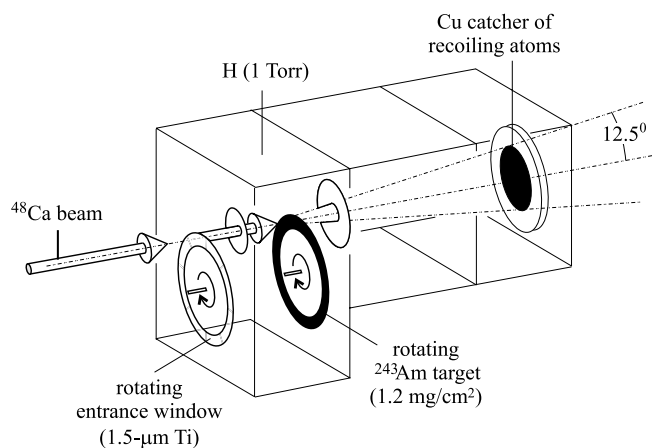


FIG. 7. Diagram of the setup for the chemical separation of the SF isotope  $^{268}\text{Db}$  produced in the reaction  $^{243}\text{Am} + ^{48}\text{Ca}$  [15,16].

50-mm-diameter copper block positioned on the beam axis, 100 mm downstream from the target. The collection efficiency of reaction products from the fusion of  $^{243}\text{Am}$  and  $^{48}\text{Ca}$  nuclei was close to 100% (acceptance angle of  $\pm 12.5^\circ$ ). The range of the recoils in the catcher did not exceed 3–4  $\mu\text{m}$ . After the end of each irradiation, a 7- to 10- $\mu\text{m}$  catcher layer (120–180 mg of Cu) was cut from the surface using a microlathe. The copper chips were dissolved in 10 ml of concentrated  $\text{HNO}_3$ .

The resulting nitric acid solution contained a large amount of copper (the catcher material), unwanted reaction products from transfer, fusion-fission, and induced fission reactions with the  $^{243}\text{Am}$  target, as well as products of the reaction of  $^{48}\text{Ca}$  with Cu. To monitor the performance of the chemical procedure for the isolation of the group 5 elements and to determine the suppression factor of the actinides, aliquots of nitrate tracer solutions containing  $^{92\text{m}}\text{Nb}$ ,  $^{177}\text{Ta}$ ,  $^{89}\text{Zr}$ ,  $^{175}\text{Hf}$ , and the rare-earth isotopes  $^{169}\text{Yb}$  and  $^{167}\text{Tm}$  were added to the solution of dissolved reaction products. The group 4/5 elements were separated from the Cu via coprecipitation with  $\text{La}(\text{OH})_3$  by introducing ammonium hydroxide and  $\text{La}^{3+}$  carrier (0.7 mg) to the solution. The precipitate was dissolved in 2 M  $\text{HNO}_3$ , which was loaded onto the strongly acidic cation exchanger DOWEX 50 $\times$ 8 and subsequently washed with 1 M HF. This procedure elutes the group 4 and 5 elements while the actinides remain adsorbed on the column. Chemical yields for group 4/5 elements of 60–80% were found, whereas actinides were suppressed by a factor of  $\geq 10^5$ . Elements with higher group numbers (6–14) were not found in the final samples due to their different chemical properties. The details of the separation procedure and model studies are described in [15,16].

In the final step of the chemical procedure, the column eluate was evaporated to a volume of 0.1 ml and deposited onto a polyethylene foil (0.4- $\mu\text{m}$  thick, 15 mm in diameter) with subsequent drying in a stream of warm helium. All procedures starting from the end of irradiation until the beginning of detector measurements took 2–3 h.

For the registration of  $\alpha$  particles and SF fragments, we used a detection module with four identical chambers, each with two semiconductor detectors. Each individual detector

TABLE III. Parameters and results of the chemical experiments [15,16].

Run	Irradiation time (h)	Beam dose in $10^{17}$	$E_1/E_2$ (MeV)	Neutron count	Registration time (h)
1	20	2.5	120/126	2	20
2	22	3.7	—/86	1	74
3	22	3.4	131/124	1	15
			116/122	2	72
4	22	2.9	104/120	1	22
			97/125	1	29
			100/128	1	51
			117/118	2	6
5	38	6.7	108/107	3	9
			110/104	0	15
			—/76	2	68
			120/114	2	39
6	23	3.9	—	—	—
7	22	3.6	—	—	—
8	45	7.4	119/110	2	5
			118/105	2	93
			65/58	3	174

had a surface area of  $6 \text{ cm}^2$ . In each chamber, two detectors were mounted facing each other, separated by a 4-mm gap. The sample under study was placed between the two detectors in each chamber. Four of the chambers were located inside a neutron detector for the registration of SF neutrons. The neutron detector had 72  $^3\text{He}$  counters that were distributed in a polyethylene moderator as three concentric rings at different distances from the chambers with the counting samples. The detector array was calibrated with  $^{248}\text{Cm}$  and  $^{252}\text{Cf}$  sources. The efficiency for the detection of fission fragments with the semiconductor detectors was about 90%; neutrons were detected with an average efficiency of about 40% [39]. The average counting rate of single background neutrons was  $30 \text{ s}^{-1}$ . Neutron signals were acquired during a  $100\text{-}\mu\text{s}$  gate opened by a fission event; thus the detection probability of random neutrons in coincidence with any SF signal was  $3 \times 10^{-3}$ . During the experiment, as newer samples were placed in the detection module with the neutron detector, older samples were placed in a similar, yet separate, detection module without a neutron detector to continue counting. In the course of the 330-h test run performed before the experiment, no background SF events were detected.

The experiment designed to identify  $^{268}\text{Db}$  produced via the  $^{243}\text{Am}(^{48}\text{Ca}, 3n)^{288}\text{115}$  reaction was performed between June 11 and 22, 2004 [15,16]. A total of eight similar irradiations, lasting between 20 and 45 h each, were performed. With irradiations of this length, we could count on the effective registration of decays of nuclides with half-lives  $T_{1/2} \geq 10 \text{ h}$ .

The target was bombarded by  $^{48}\text{Ca}$  ions with an energy corresponding to 247 MeV in the middle of the target; the resulting excitation energy of the compound nucleus  $^{291}\text{115}$  was  $E^* = 35.0\text{--}43.8 \text{ MeV}$ , covering practically the entire energy interval of the  $3n$ -evaporation channel of the  $^{243}\text{Am} + ^{48}\text{Ca}$  reaction leading to the isotope  $^{288}\text{115}$ . A total beam dose of  $3.4 \times 10^{18}$   $^{48}\text{Ca}$  projectiles was collected in this experiment.

During the counting following the eight irradiations of the  $^{243}\text{Am}$  target with  $^{48}\text{Ca}$  ions, 15 SF events were detected. The measurements were carried out for a total of 957 h. All SF events appeared in a 174-h interval following the start of the measurements. No SF events were detected in the subsequent 783 h. Table III gives the run conditions and the results of the measurements (fission fragment energies corrected for losses in the source and backing layer, numbers of neutrons detected by the  $^3\text{He}$  counters for every fission event, and registration times of SF events from the beginning of the measurement of that particular sample).

A ninth irradiation was carried out under the same conditions, with the same beam energy as in the previous eight runs, but *without chemical separation* of the reaction products. The goal of this experiment was to determine the background of spontaneously fissioning nuclei (mainly Cf isotopes) implanted into the catcher. After the end of the 19-h irradiation (with a  $^{48}\text{Ca}$  ion beam dose of  $2.9 \times 10^{17}$ ) the catcher was put in contact with a solid-state track detector. During the course of a 72-d exposure, the detectors were changed at regular intervals and subjected to a physical-chemical treatment to develop the latent tracks of SF fragments. A total of 158 tracks were observed; the detection rate of about 2 events per day was virtually unchanged throughout the duration of counting. With a chemical separation factor of group 5 elements from actinides of  $\geq 10^5$ , the spontaneous fission of all actinide isotopes, including  $^{252,254}\text{Cf}$  and  $^{264}\text{Lr}$ , could yield no more than  $2 \times 10^{-3}$  events in 174 h.

The method used for chemical separation possesses a high selectivity for the elements of groups 4 and 5. Therefore, it is necessary to determine the possible quantity (or upper limit) for the group 4 elements (e.g., Rf isotopes,  $Z = 104$ ) in the solution. In the reaction  $^{243}\text{Am} + ^{48}\text{Ca}$ , they can be produced via the  $p xn$  channel as descendant nuclei of the element 114 isotopes,  $^{243}\text{Am}(^{48}\text{Ca}, p xn)^{290-x}\text{114}$ . Any isotopes of element 114 that should undergo five consecutive  $\alpha$  decays would

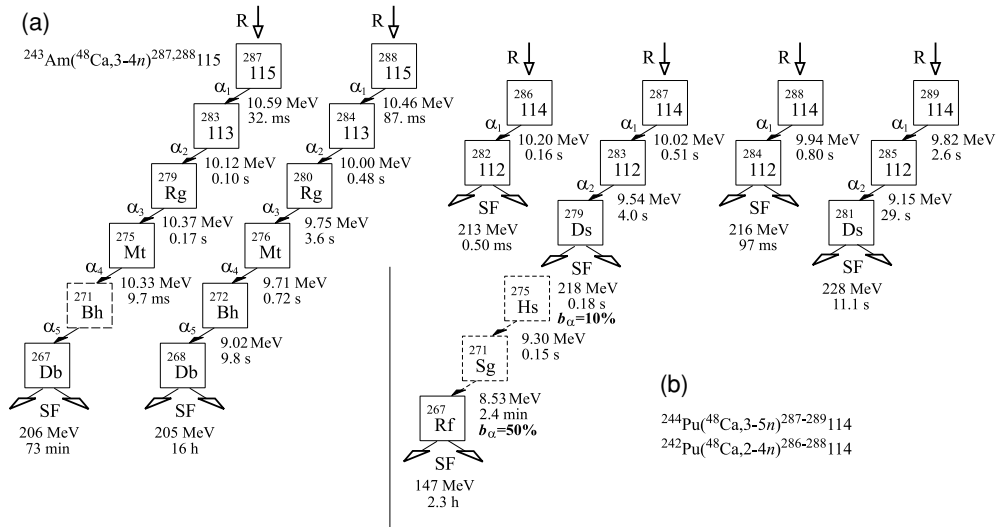


FIG. 8. Time sequences in the decay chains observed in the  $^{243}\text{Am} + ^{48}\text{Ca}$  reaction (a) and of isotopes with  $Z = 114$  produced in reactions with even- $Z$  targets (b). The measured energies and half-lives of the observed nuclei are shown. Branching ratios  $b_\alpha$  are given for nuclei if both  $\alpha$  decay and spontaneous fission were registered.

lead to the production of isotopes of element 104. Despite the low expected competition of the  $p\alpha n$ -reaction channel in comparison with the  $xn$  channel (previously mentioned), we must consider the decay properties of the element 114 isotopes.

The reactions  $^{242,244}\text{Pu} + ^{48}\text{Ca}$  leading to the compound nuclei  $^{290}\text{114}$  and  $^{292}\text{114}$ , which have one proton less than  $^{291}\text{115}$  and at least the same number of neutrons, are significant for this purpose. The decay chains of  $^{286-289}\text{114}$  are shown in Fig. 8; their cross sections have been measured over a wide range of projectile energies and they have been produced in cross bombardments as well [1,2].

The decay chains of all these isotopes with  $Z = 114$  lasted only 0.02–170 s and were terminated by spontaneous fission of nuclei with  $Z = 112$  or 110 depending on whether or not all of the neutrons in the parent even- $Z$  nucleus were paired. In only one of 25 decay chains containing the nuclide  $^{279}\text{Ds}$  did

we observe a long  $\alpha$  decay chain,  $^{279}\text{Ds}(\alpha) \rightarrow ^{275}\text{Hs}(\alpha) \rightarrow ^{271}\text{Sg}(\alpha) \rightarrow ^{267}\text{Rf}(\text{SF})$ , leading to a SF isotope with  $T_{\text{SF}} \approx 2.3$  h. The detection probability for this rare  $\alpha$ -decay branch of  $^{279}\text{Ds}$  in the chemistry experiment is  $2 \times 10^{-3}$  due to saturation during the time durations of the bombardments, chemical separations, and measurements of samples. In fact, this limit is even lower because in the on-line reaction  $^{243}\text{Am} + ^{48}\text{Ca}$ , at a total beam dose of  $0.9 \times 10^{19}$ , we observed no isotopes of element 114 that could be the products of the  $p\alpha n$ -reaction channel for  $1 \leq x \leq 4$ . Therefore, all 15 SF events observed in the chemistry experiment are assigned to the decay of the group 5 nuclide with  $Z = 105$ .

The parameters of both the DGFRS and chemistry experiments and the decay properties of the final SF nuclide observed after five consecutive  $\alpha$  decays in the  $^{243}\text{Am} + ^{48}\text{Ca}$  reaction are presented in Table IV. Over the course of the chemistry experiment, 15 SF decays were observed with  $T_{1/2} = 32^{+11}_{-7}$  h

TABLE IV. Parameters and results of the DGFRS [3] and chemical experiments [15,16].

Separation method	DGFRS experiment Recoil separator	Chemical experiment Radiochemical separation
Separation efficiency	35%	80%
Detection method	Decay chains of nuclei with $Z = 115$	SF of nuclei with $Z = 105$
$^{48}\text{Ca}$ beam energy in the middle of target layer	246 MeV	247 MeV
Total $^{48}\text{Ca}$ beam dose	$4.3 \times 10^{18}$	$3.4 \times 10^{18}$
Thickness of the $^{243}\text{Am}$ target	0.36 mg/cm <sup>2</sup>	1.2 mg/cm <sup>2</sup>
Number of detected SF events	3	15
Formation cross section for the nuclei with $Z = 115$	$2.7^{+4.8}_{-1.6}$ pb	$4.2^{+1.6}_{-1.2}$ pb
Half-life	$16^{+19}_{-6}$ h	$32^{+11}_{-7}$ h
Total kinetic energy of fission fragments	$\approx 225$ MeV	$\approx 230$ MeV
Average neutron multiplicity per fission	—	4.2
Identification method of SF-decaying nuclei in the reaction $^{243}\text{Am} + ^{48}\text{Ca}$	Measurement of excitation functions ( $Z = 115$ )	Isolation of group 5 elements ( $Z = 105$ )

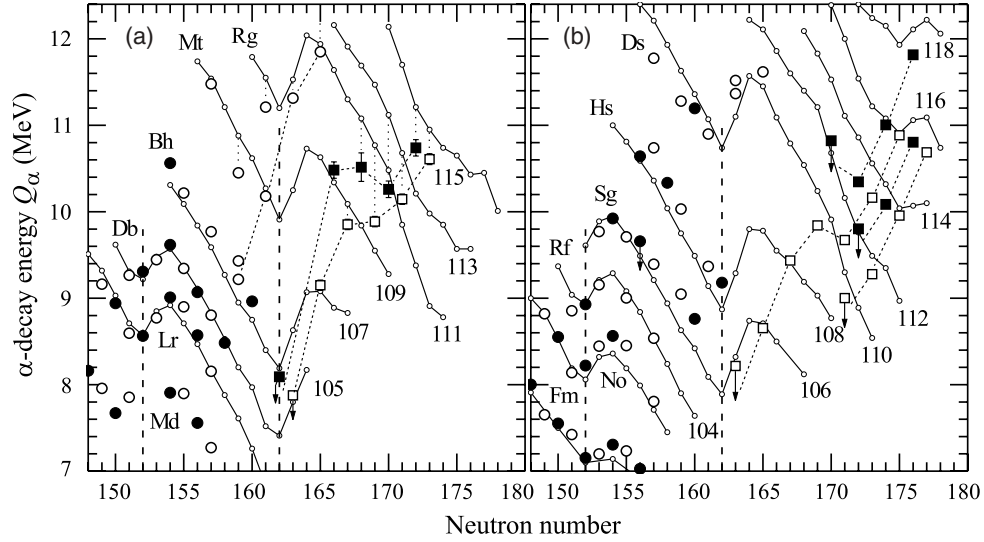


FIG. 9. (a)  $\alpha$ -decay energy vs neutron number for isotopes of odd- $Z$  elements with  $Z \geq 101$  (solid circles, odd-even isotopes; open circles, odd-odd isotopes) [8–10,28,31–33,35,40–46]. Data at  $N \geq 162$  that are connected by dashed lines are from [1–3,20] and the present work (squares). Solid lines show the theoretical  $Q_\alpha$  values [6,7,47] for odd  $Z = 103$ –115 elements. (b) The same for even- $Z$  elements.

and total deposited energy  $E_{\text{tot}} \approx 230$  MeV [15,16]. The production cross section for this SF activity in the  $^{243}\text{Am} + ^{48}\text{Ca}$  reaction was  $4.2^{+1.6}_{-1.2}$  pb. These results agree with the original element 115 synthesis experiment with DGFRS where the same SF activity ( $T_{1/2} = 16^{+19}_{-6}$  h,  $E_{\text{tot}} \approx 225$  MeV,  $\sigma_{3n} = 2.7^{+4.8}_{-1.6}$  pb determined for three observed events) was first observed as the terminal isotope following the five consecutive  $\alpha$  decays from the  $^{288}\text{115}$  parent nucleus.

Thus, the data from the chemistry experiment give independent evidence for the synthesis of element 115, as well as element 113, via the  $^{243}\text{Am} + ^{48}\text{Ca}$  reaction.

## V. DISCUSSION

The experimental  $\alpha$ -decay energies  $Q_\alpha^{\text{exp}}$  of the synthesized isotopes and previously known odd- $Z$  nuclei with  $Z \geq 103$  are plotted in Fig. 9(a). The  $Q_\alpha^{\text{exp}}$  of even- $Z$  nuclei, including those produced in our experiments [1,2,20], are plotted in Fig. 9(b) for comparison. The  $\alpha$ -decay energies attributed to the isotopes of Mt and Bh coincide well with theoretical values [7], also plotted in the figures. The same can be seen for the last nuclei in the decay chain  $^{275}\text{Hs} \rightarrow ^{271}\text{Sg} \rightarrow ^{267}\text{Rf}$ .

The trend of the  $Q_\alpha(N)$  systematics predicted by the MM model [6,7] and confirmed by experimental data for odd- $Z$  isotopes of Mt and Bh along with even- $Z$  isotopes of Ds can be considered as direct experimental evidence for the deformed neutron shell closure at  $N = 162$ . The stabilizing effect of the  $N = 162$  shell can be seen for Db isotopes. The relatively small change in the half-lives of known lighter mass isotopes  $^{260}\text{Db}$  ( $T_{1/2} = 1.5$  s),  $^{261}\text{Db}$  ( $T_{1/2} = 1.8$  s),  $^{262}\text{Db}$  ( $T_{1/2} = 34$  s), and  $^{263}\text{Db}$  ( $T_{1/2} = 27$  s) [28] contributes to the prediction of a considerable increase in  $T_\alpha$  for the new heavier isotopes  $^{267}\text{Db}$  and  $^{268}\text{Db}$  with  $T_\alpha \geq 5 \times 10^3$  s and  $T_\alpha \geq 3 \times 10^5$  s, respectively.

The parent and daughter nuclei,  $^{288}\text{115}$  ( $N = 173$ ) and  $^{284}\text{113}$  ( $N = 171$ ), are rather distant from the deformed shell

at  $N = 162$ , so their relatively long half-lives could be caused by the influence of the next spherical shell at  $N = 184$ . The comparison of the decay properties of the odd-odd isotope  $^{278}\text{113}$  ( $N = 165$ ) observed in one decay chain produced recently in the cold fusion reaction  $^{209}\text{Bi}(^{70}\text{Zn}, 1n)^{278}\text{113}$  [48] with those for  $^{284}\text{113}$  ( $N = 171$ ) reveals a decrease of  $\alpha$ -decay energy by 1.7 MeV and a corresponding increase in half-life by a factor of  $2 \times 10^3$  because of closer proximity to the region of spherical nuclei. The odd-odd isotopes,  $^{272}\text{Rg}$  ( $T_{1/2} = 3.1$  ms) [8–10],  $^{274}\text{Rg}$  ( $T_{1/2} = 6.4$  ms) [48], and  $^{280}\text{Rg}$  ( $T_{1/2} = 3.6$  s), demonstrate comparable behavior.

For the isotopes  $^{279,280}\text{Rg}$  and  $^{283,284}\text{113}$  the difference between theoretical and experimental  $Q_\alpha$  values is 0.6–0.9 MeV. Some part of this energy can be accounted for by  $\gamma$ -ray emission from excited levels populated during  $\alpha$  decay. For the even- $Z$  nuclei as well, the agreement between theory and experiment becomes somewhat worse as one moves from the deformed nuclei in the vicinity of neutron shells  $N = 152$  and  $N = 162$  to the more neutron-rich nuclides with  $N \geq 169$ . In this region, experimentally measured values of  $Q_\alpha$  are less than the values calculated from the model by  $\leq 0.5$  MeV. Although the predicted  $Q_\alpha$  values for the heaviest nuclei observed in our experiments are systematically larger than the experimental data as a whole, the trends of the predictions are in good agreement for the 23 nuclides with  $Z = 106$ –118 and  $N = 165$ –177, especially considering that the theoretical predictions of the MM model match the experimental data over a broad previously unexplored region of nuclides.

One should note that the predictions of other models for even- $Z$  and odd- $Z$  nuclei within the Skyrme-Hartree-Fock-Bogoliubov [12,49–51] and the relativistic mean-field [13,52–57] methods also compare well with the experimental results. These models predict the same spherical neutron shell at  $N = 184$ , but different proton shells,  $Z = 114$  (MM) and  $Z = 120, 124$ , or  $126$  (SHFB, RMF), yet all describe the experimental data equally well. Such insensitivity with respect

TABLE V. Decay properties of nuclei produced in the reaction  $^{243}\text{Am} + ^{48}\text{Ca}$ .

Isotope	Decay mode	Half-life <sup>a</sup>	$E_\alpha$ (MeV)	$Q_\alpha$ (MeV)	Isotope	Decay mode	Half-life <sup>a</sup>	$E_\alpha$ (MeV)	$Q_\alpha$ (MeV)
$^{288}\text{115}$	$\alpha$	$87^{+105}_{-30}$ ms (60 ms)	$10.46 \pm 0.06$	$10.61 \pm 0.06$	$^{287}\text{115}$	$\alpha$	$32^{+155}_{-14}$ ms (30 ms)	$10.59 \pm 0.09$	$10.74 \pm 0.09$
$^{284}\text{113}$	$\alpha$	$0.48^{+0.58}_{-0.17}$ s (0.3 s)	$10.00 \pm 0.06$	$10.15 \pm 0.06$	$^{283}\text{113}$	$\alpha$	$100^{+490}_{-45}$ ms (140 ms)	$10.12 \pm 0.09$	$10.26 \pm 0.09$
$^{280}\text{Rg}$	$\alpha$	$3.6^{+4.3}_{-1.3}$ s (0.4 s)	$9.75 \pm 0.06$	$9.87 \pm 0.06$	$^{279}\text{Rg}$	$\alpha$	$170^{+810}_{-80}$ ms (7 ms)	$10.37 \pm 0.16$	$10.52 \pm 0.16$
$^{276}\text{Mt}$	$\alpha$	$0.72^{+0.87}_{-0.25}$ s (0.1 s)	$9.71 \pm 0.06$	$9.85 \pm 0.06$	$^{275}\text{Mt}$	$\alpha$	$9.7^{+46}_{-4.4}$ ms (2 ms)	$10.33 \pm 0.09$	$10.48 \pm 0.09$
$^{272}\text{Bh}$	$\alpha$	$9.8^{+11.7}_{-3.5}$ s (3 s)	$9.02 \pm 0.06$	$9.15 \pm 0.06$	$^{271}\text{Bh}$	$\alpha$	$\overline{(\overline{5} \text{ s})}$	—	$9.07^b$
$^{268}\text{Db}$	SF/EC	$29^{+9}_{-6}$ h (6 h)		$7.80^b$	$^{267}\text{Db}$	SF	$73^{+350}_{-33}$ min (9 d)		$7.41^b$

<sup>a</sup>Error bars correspond to 68% confidence level. Expected half-lives for allowed transitions shown in parenthesis were calculated using formula by Viola and Seaborg [58] and measured or predicted [7]  $Q_\alpha$  values.

<sup>b</sup>Calculated values by Muntian *et al.* [7].

to the various models in this region of  $Z$  and  $N$  can be explained either by the remoteness of nuclei under consideration from the closed shell at  $N = 184$  or by the weaker influence of the proton shells at  $Z = 114$  or higher, compared with that of the neutron shell at  $N = 184$ .

For the measured  $\alpha$ -decay energies of the new isotopes, one can estimate half-lives for *allowed transitions* and compare them with experimental values under the Geiger-Nuttall treatment using the formula by Viola and Seaborg [58]:  $\log_{10}(T_\alpha) = (aZ + b)^* Q_\alpha^{-1/2} + cZ + d$ . Parameters were fitted to the  $T_\alpha$  versus  $Q_\alpha$  values of 65 previously known even-even nuclei with  $Z > 82$  and  $N > 126$  ( $a = 1.787$ ,  $b = -21.40$ ,  $c = -0.2549$ ,  $d = -28.42$ ). The limiting values of  $Q_\alpha$  for the spontaneously fissioning nuclei were estimated in the same way. The ratios between experimental  $T_{\text{exp}}$  and calculated  $T_{\text{calc}}$  half-lives (see Table V) define the hindrance factors caused by odd numbers of protons and/or neutrons in the newly synthesized nuclei. The measured  $T_{\text{exp}}$  values closely reproduce the calculated ones for the first two nuclei of these chains; thus the element 115 and element 113 isotopes have rather low hindrance factors, if any, for  $\alpha$  decay. For the isotopes of elements Rg, Mt, and Bh, the difference between measured and calculated  $T_\alpha$  values results in hindrance factors of 3–10. These match the hindrance factors that can be extracted for the deformed odd-odd nuclei  $^{272}\text{Rg}$  and descendants produced in experiments at GSI [8,9] and RIKEN [10]. One can suppose that, in this region of nuclei, a noticeable transition from spherical to deformed shapes occurs at  $Z = 109$ –111, resulting in the complication of the level structures of these nuclei and in an increased probability of  $\alpha$  transitions going through excited states. Another sign of such a shape change might be the significant increase in the difference of  $\alpha$ -decay energies of the neighboring isotopes observed as the decay chains reach  $Z = 111$  [see Fig. 9(a)]. This assumption is in agreement with MM calculations [6,7]. The deformation parameter  $\beta_2$  was calculated to be 0.072 and 0.138 for  $^{288}\text{115}$  and  $^{284}\text{113}$ , respectively (see Fig. 1). As

the decay chain recedes from the shell closure at  $Z = 114$ , the deformation parameter  $\beta_2$  increases to 0.200, 0.211, and 0.247 for  $^{280}\text{Rg}$ ,  $^{276}\text{Mt}$ , and  $^{272}\text{Bh}$ , respectively. In the decay chain  $^{291}\text{116} \rightarrow \dots \rightarrow ^{267}\text{Rf}$  [Fig. 9(b)], we observed a similar variation in  $\alpha$ -decay energies. The slope of  $Q_\alpha$  versus neutron number remains practically the same for elements 112–116 but increases significantly for the nuclides with  $Z = 111$  and 110. Again, such an effect might be caused by the transition from spherical nuclear shapes to deformed shapes during successive  $\alpha$  decays, in agreement with MM calculations [6,7].

The hindrance to SF caused by the odd proton allows the odd- $Z$  nuclei to undergo consecutive  $\alpha$  decays leading to the elements 105–107 that have a large neutron excess. The number of neutrons in such nuclides can be varied downward by using other target nuclei (e.g.,  $^{241}\text{Am}$ ,  $^{237}\text{Np}$ , or  $^{231}\text{Pa}$ ). Therefore, the investigation of the region of nuclei located near deformed shell closures  $Z = 108$  and  $N = 162$  that has been explored from the  $N < 162$  side in the cold fusion reactions (see, e.g., Refs. [8–10,35] and references therein) now can be approached from the high- $N$  side using  $^{48}\text{Ca}$ -induced reactions. Note also that the rather long lifetimes of Db isotopes permit us to investigate in more detail the chemical properties of this element, previously studied only in on-line experiments with the short-lived isotopes  $^{261,262,263}\text{Db}$  ( $T_\alpha = 1.8$ , 34, and 27 s) (see, e.g. [37,38,59,60] and references therein).

The decay properties of nuclei observed in the decay chains terminated by isotopes  $^{267}\text{Db}$  and  $^{268}\text{Db}$  are presented in Table V. The  $\alpha$ -decay branching ratio should be low for  $^{268}\text{Db}$  because for its  $\alpha$ -decay product,  $^{264}\text{Lr}$ , one would expect a rather long half-life ( $Q_\alpha = 6.84$  MeV [7],  $T_\alpha \geq 100$  d;  $Q_{\text{EC}} = 0.050$  MeV [29],  $T_{\text{EC}} \geq 100$  d [30];  $T_{\text{SF}} \geq 10$  d (see, e.g. [11] and  $T_{\text{SF}}$  for neighboring Lr isotopes)). The same conclusion follows from the results of our subsequent chemistry experiments (see previous discussion). Comparing the cross section values measured in the DGFRS and chemistry experiments for the SF activity, one can suppose that the  $\alpha$  decay of  $^{268}\text{Db}$  with a half-life less than 10 h seems to be

improbable, which is in agreement with the conclusion drawn here. The calculations of the upper limit for the  $\alpha$ -decay energy of  $^{268}\text{Db}$  using the sum value  $T_{1/2} = 29^{+9}_{-6}$  h determined from 18 events and a possible hindrance factor for the  $\alpha$  decay of an odd-odd isotope of 30 results in the value  $Q_\alpha \leq 7.88$  MeV, which is rather close to the predicted value  $Q_\alpha = 7.80$  MeV [7]. This would indicate that an  $\alpha$  decay branch of no more than 25% was possible for  $^{268}\text{Db}$ .

It cannot be excluded that  $^{268}\text{Db}$  undergoes electron capture ( $Q_{\text{EC}} = 1.68$  MeV [29],  $T_{\text{EC}} \sim 20$  h [30]) and the observed SF events originate from its short-lived descendant, even-even isotope  $^{268}\text{Rf}$  ( $T_{\text{SF}} = 1.4$  s [11],  $Q_\alpha = 7.64$  MeV [61],  $T_\alpha \sim 10$  h). However, that does not change the conclusions made here. Since both  $^{268}\text{Db}$  and  $^{268}\text{Rf}$  would yield symmetric fission fragments close to the  $Z = 50$  and  $N = 82$  spherical shells, one would expect their SF decays to result in symmetric mass distributions of fission fragments with rather high total kinetic energies.

The TKE for all heavy nuclides with  $Z \geq 105$  produced in  $^{48}\text{Ca}$ -induced reactions [1–3,20] is plotted in Fig. 10, together with the previously known data for isotopes with  $Z \geq 96$  (see Ref. [62] and references therein). The total kinetic energy of the fission fragments of  $^{268}\text{Db}$  ( $^{268}\text{Rf}$ ), determined in the chemistry experiment as the sum of amplitudes of the time-coincident signals from both detectors, and corrected for energy loss in the source and backing layers, was 230 MeV.

It is observed that, with an onset at  $Z \geq 110$ , the TKE smoothly increases with increasing  $Z$  in agreement with the

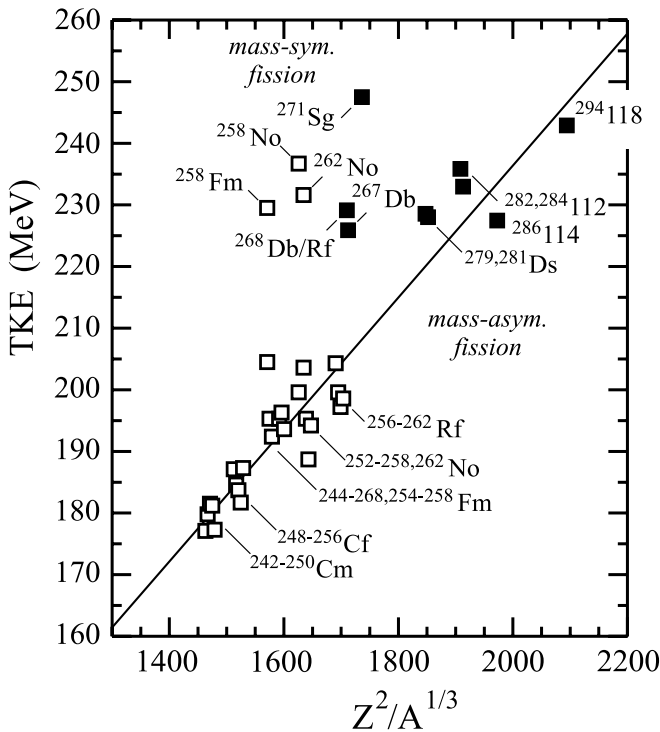


FIG. 10. Experimental values of TKE vs  $Z^2/A^{1/3}$  (measured data from [62] and references therein, open squares; experimental data for heaviest nuclei [1–3] including data from the present work, solid squares). The line is the linear fit to the data, excluding the mass-symmetric fissioners [63].

dependence of TKE versus  $Z^2/A^{1/3}$ , typical for asymmetric fission of the lighter nuclides. We consider that this is caused by the influence of the spherical shells  $Z = 50$  and  $N = 82$  on the formation of the light fission fragment in the scission of superheavy nuclei (see Refs. [62,64,65] and references therein). In the SF of the lighter nuclides  $^{267}\text{Db}$ ,  $^{268}\text{Db}$  ( $^{268}\text{Rf}$ ), and  $^{271}\text{Sg}$  with  $N = 162$ , 163, and 165, the same effect apparently results in symmetric fission with high kinetic energy, characteristic of the close scission configuration that takes place in the bimodal fission of the heavy isotopes of Fm, Md, and No [62,65]. Mass symmetry of the fission fragments ( $E_{F1}/E_{F2} \sim 1$ ) and the high TKE and neutron multiplicity of  $^{268}\text{Db}$  ( $^{268}\text{Rf}$ ) measured in the chemistry experiment are consistent with a calculated total energy release for symmetric fission of  $Q_{\text{SF}} \approx 280$  MeV [29].

## VI. CONCLUSION

Several conclusions follow from our analysis and discussion of the present experimental data [3,15,16]. In the  $^{243}\text{Am} + ^{48}\text{Ca}$  reaction two new elements with atomic numbers 113 and 115 were observed for the first time. The decay properties were determined for two isotopes,  $^{288}115$  and  $^{287}115$ , produced in the  $3n$ - and  $4n$ -evaporation channels of the reaction with cross sections of about 4 pb and 1 pb, respectively. These new nuclides undergo consecutive  $\alpha$  decays terminated by spontaneous fission. In the decay chain of the odd-odd isotope  $^{288}115$ , five sequential  $\alpha$  transitions last about 30 s, whereas the half-life of  $^{268}\text{Db}$  is about 30 h.

The atomic numbers of all nuclei in the decay chain of  $^{288}115$  ( $Z = 115 \rightarrow Z = 113 \rightarrow Z = 111 \rightarrow Z = 109 \rightarrow Z = 107 \rightarrow Z = 105$ ) were also determined in an independent experiment by chemical identification of the final SF nucleus. It was shown that spontaneous fission is due to the decay (SF or EC-SF) of  $^{268}\text{Db}$  ( $Z = 105$ ), a member of the fifth group of the Periodic Table.

The production cross section of element 115 in the reaction  $^{243}\text{Am} + ^{48}\text{Ca}$  exceeds that of the lighter isotope of element 113 in the cold fusion reaction  $^{209}\text{Bi} + ^{70}\text{Zn}$  by two orders of magnitude. The decay properties of 11 new isotopes with  $Z = 105$ –115 and their production cross sections in the reaction of  $^{243}\text{Am}$  with  $^{48}\text{Ca}$  are in agreement with the modern concepts on the role of nuclear shells in the stability of heavy and superheavy nuclei.

## ACKNOWLEDGMENTS

We are indebted to Profs. W. Greiner, S. Hofmann, A. Sobczewski, and B. F. Myasoedov for interesting discussions and valuable comments.

We are grateful to the JINR directorate, in particular to Profs. V. G. Kadyshevsky, A. N. Sissakian, and Ts. Vylov for the help and support we received during all stages of the experiment.

This work has been performed with the support of the Russian Ministry of Atomic Energy, RFBR grant Nos. 04-02-17186 and 04-03-32047, and the Swiss National Scientific Foundation. Much of the support for the LLNL authors

was provided through the U.S. DOE under Contract No. W-7405-Eng-48. The  $^{243}\text{Am}$  target material was provided by RIAR, Dimitrovgrad, and by the U.S. DOE through ORNL.

These studies were performed in the framework of the Russian Federation/U.S. Joint Coordinating Committee for Research on Fundamental Properties of Matter.

- 
- [1] Yu. Ts. Oganessian *et al.*, Phys. Rev. C **62**, 041604(R) (2000); Phys. At. Nucl. **63**, 1679 (2000); Phys. Rev. C **63**, 011301(R) (2001); Phys. At. Nucl. **64**, 1349 (2001); Eur. Phys. J. A **15**, 201 (2002).
- [2] Yu. Ts. Oganessian *et al.*, Phys. Rev. C **69**, 054607 (2004); Nucl. Phys. A **734**, 109 (2004); Phys. Rev. C **70**, 064609 (2004).
- [3] Yu. Ts. Oganessian *et al.*, Phys. Rev. C **69**, 021601(R) (2004).
- [4] V. I. Zagrebaev, M. G. Itkis, and Yu. Ts. Oganessian, Phys. At. Nucl. **66**, 1033 (2003).
- [5] V. I. Zagrebaev, in *Proceedings of the Tours Symposium on Nuclear Physics V, Tours, France, 2003* (American Institute of Physics, New York, 2004), p. 31; Nucl. Phys. A **734**, 164 (2004).
- [6] I. Muntian, Z. Patyk, and A. Sobiczewski, Phys. At. Nucl. **66**, 1015 (2003).
- [7] I. Muntian *et al.*, Acta Phys. Pol. B **34**, 2073 (2003).
- [8] S. Hofmann *et al.*, Z. Phys. A **350**, 281 (1995).
- [9] S. Hofmann *et al.*, Eur. Phys. J. A **14**, 147 (2002).
- [10] K. Morita *et al.*, J. Phys. Soc. Jpn. **73**, 1738 (2004).
- [11] R. Smolańczuk, J. Skalski, and A. Sobiczewski, Phys. Rev. C **52**, 1871 (1995).
- [12] S. Goriely *et al.*, Phys. Rev. C **66**, 024326 (2002).
- [13] Z. Ren *et al.*, Phys. Rev. C **67**, 064302 (2003).
- [14] S. N. Dmitriev, Yu. Ts. Oganessian, and M. G. Itkis, in *Proceedings of the Second International Conference on the Chemistry and Physics of Transactinide Elements, Extended Abstracts, TAN 03, Napa, California, USA, 2003*, LBNL-53896 Abs., [www.tan03.lbl.gov](http://www.tan03.lbl.gov), p. 204.
- [15] S. N. Dmitriev *et al.*, Mendelev Commun. **1** (2005); S. N. Dmitriev *et al.*, in *Proceedings of the International Symposium on Exotic Nuclei, EXON 2004, Peterhof, Russia, 2004*, edited by Yu. E. Penionzhkevich and E. A. Cherepanov (World Scientific, Singapore, 2005), p. 285; JINR Preprint E12-2004-157 (2004) [[http://www.jinr.ru/publish/Preprints/2004/157\(e12-2004-157\).pdf](http://www.jinr.ru/publish/Preprints/2004/157(e12-2004-157).pdf)].
- [16] D. Schumann *et al.*, Radiochim. Acta **93**, 1 (2005).
- [17] Yu. Ts. Oganessian *et al.*, in *Proceedings of the Fourth International Conference on Dynamical Aspects of Nuclear Fission, Častá-Papiernička, Slovak Republic, 1998* (World Scientific, Singapore, 2000), p. 334; K. Subotic *et al.*, Nucl. Instrum. Methods Phys. Res. A **481**, 71 (2002).
- [18] V. G. Subbotin *et al.*, Acta Phys. Pol. B **34**, 2159 (2003); Yu. S. Tsyganov *et al.*, Nucl. Instrum. Methods Phys. Res. A **525**, 213 (2004).
- [19] Yu. Ts. Oganessian *et al.*, Phys. Rev. C **64**, 064309 (2001).
- [20] Yu. Ts. Oganessian *et al.*, JINR Communication D7-2002-287 2002 [[http://www.jinr.ru/publish/Preprints/2002/287\(D7-2002-287\)e.pdf](http://www.jinr.ru/publish/Preprints/2002/287(D7-2002-287)e.pdf)] (unpublished); Lawrence Livermore National Laboratory Report UCRL-ID-151619, 2003 (unpublished).
- [21] N. J. Stoyer *et al.*, Nucl. Instrum. Methods Phys. Res. A **455**, 433 (2000).
- [22] R. Bass, in *Proceedings of the Symposium on Deep Inelastic and Fusion Reactions with Heavy Ions, West Berlin, 1979*, edited by W. von Oertzen, Lecture Notes in Physics, Vol. 117 (Springer-Verlag, Berlin, 1980), p. 281.
- [23] W. D. Myers and W. J. Swiatecki, Nucl. Phys. A **601**, 141 (1996).
- [24] F. Hubert, R. Bimbot, and H. Gauvin, At. Data Nucl. Data Tables **46**, 1 (1990).
- [25] L. C. Northcliffe and R. F. Schilling, Nucl. Data Tables A **7**, 233 (1970).
- [26] K.-H. Schmidt *et al.*, Z. Phys. A **316**, 19 (1984).
- [27] V. B. Zlokazov, Eur. Phys. J. A **8**, 81 (2000).
- [28] *Table of Isotopes*, 8th ed., edited by R. B. Firestone and V. S. Shirley (Wiley, New York, 1996).
- [29] G. Audi, A. H. Wapstra, and C. Thibault, Nucl. Phys. A **729**, 337 (2003).
- [30] N. N. Kolesnikov, A. P. Krylova, and V. K. Kandybarov, Izv. Acad. Nauk SSSR, Ser. Fiz. **27**, 132 (1963); N. N. Kolesnikov and A. G. Demin, JINR Communication P6-9421, 1975 (in Russian; unpublished).
- [31] Yu. A. Lazarev *et al.*, Phys. Rev. Lett. **73**, 624 (1994).
- [32] Yu. A. Lazarev *et al.*, Phys. Rev. Lett. **75**, 1903 (1995).
- [33] Yu. A. Lazarev *et al.*, Phys. Rev. C **54**, 620 (1996).
- [34] Yu. Ts. Oganessian *et al.*, Radiochim. Acta **37**, 113 (1984).
- [35] S. Hofmann and G. Münzenberg, Rev. Mod. Phys. **72**, 733 (2000).
- [36] E. K. Hyde, I. Perlman, and G. T. Seaborg, *The Nuclear Properties of the Heavy Elements, Detailed Radioactive Properties* (Prentice-Hall, Englewood Cliffs, New Jersey, 1964).
- [37] W. Paulus *et al.*, Radiochim. Acta **84**, 69 (1999).
- [38] H. W. Gäggeler and A. Türler, in *The Chemistry of Superheavy Elements*, edited by M. Schädel (Kluwer Academic Publisher, Dordrecht, 2003), p. 237; J. V. Kratz, *ibid.* p. 159.
- [39] E. A. Sokol *et al.*, Nucl. Instrum. Methods Phys. Res. A **400**, 96 (1997).
- [40] Ch. E. Düllmann *et al.*, Nature **418**, 859 (2002).
- [41] A. Türler *et al.*, Phys. Rev. C **57**, 1648 (1998).
- [42] A. Türler *et al.*, Eur. Phys. J. A **15**, 271 (2002).
- [43] A. Türler *et al.*, Eur. Phys. J. A **17**, 505 (2003).
- [44] Z. G. Gan *et al.*, Eur. Phys. J. A **10**, 21 (2001).
- [45] P. A. Wilk *et al.*, Phys. Rev. Lett. **85**, 2697 (2000).
- [46] R. Eichler *et al.*, Nature **407**, 63 (2000).
- [47] R. Smolańczuk and A. Sobiczewski, in *Proceedings of XV Nuclear Physics Divisional Conference "Low Energy Nuclear Dynamics," St. Petersburg, Russia, 1995* (World Scientific, Singapore, 1995), p. 313; R. Smolańczuk, Phys. Rev. C **56**, 812 (1997).
- [48] K. Morita *et al.*, J. Phys. Soc. Jpn. **73**, 2593 (2004).
- [49] S. Ćwiok, W. Nazarewicz, and P. H. Heenen, Phys. Rev. Lett. **83**, 1108 (1999).
- [50] J. F. Berger, D. Hirata, and M. Girod, Acta Phys. Pol. B **34**, 1909 (2003).
- [51] S. Typel and B. A. Brown, Phys. Rev. C **67**, 034313 (2003).
- [52] M. Bender, Phys. Rev. C **61**, 031302 (2000).
- [53] P.-G. Reinhard *et al.*, in *Proceedings of the Tours Symposium on Nuclear Physics IV, Tours, France, 2000* (American Institute of Physics, New York, 2001), p. 377.
- [54] Z. Ren, Phys. Rev. C **65**, 051304(R) (2002).
- [55] S. Das and G. Gangopadhyay, J. Phys. G **30**, 957 (2004).
- [56] Z. Ren *et al.*, Phys. Rev. C **67**, 064302 (2003).
- [57] L. S. Geng, H. Toki, and J. Meng, Phys. Rev. C **68**, 061303(R) (2003).

- [58] V. E. Viola Jr. and G. T. Seaborg, *J. Inorg. Nucl. Chem.* **28**, 741 (1966).
- [59] M. Schädel, *J. Nucl. Radiochem. Sci.* **3**, 113 (2002).
- [60] J. V. Kratz, *Pure Appl. Chem.* **75**, 103 (2003).
- [61] A. Sobiczewski, I. Muntian, and Z. Patyk, *Phys. Rev. C* **63**, 034306 (2001).
- [62] D. C. Hoffman and M. R. Lane, *Radiochim. Acta* **70/71**, 135 (1995).
- [63] V. E. Viola Jr., *Nucl. Data Tables A* **1**, 391 (1966).
- [64] M. G. Itkis *et al.*, in *Proceedings of the International Workshop on Fusion Dynamics at the Extremes, Dubna, Russia, 2000*, edited by Yu. Ts. Oganessian and V. I. Zagrebaev (World Scientific, Singapore, 2001), p. 93; *J. Nuc. Radiochem. Sci. (Japan)* **3**, 57 (2002).
- [65] E. K. Hulet *et al.*, *Phys. Rev. C* **40**, 770 (1989).